A Chronometric Model of the Relationship Between Frontal Midline Theta Functional Connectivity and Human Intelligence

Anna-Lena Schubert, Dirk Hagemann,
Christoph Löffler, and Jan Rummel
Heidelberg University

Stefan Arnau
IfADo-Leibniz Research Centre for Working Environment and
Human Factors, Dortmund, Germany

Individual differences in cognitive control have been suggested to act as a domain-general bottleneck constraining performance in a variety of cognitive ability measures, including but not limited to fluid intelligence, working memory capacity, and processing speed. However, owing to psychometric problems associated with the measurement of individual differences in cognitive control, it has been challenging to empirically test the assumption that individual differences in cognitive control underlie individual differences in cognitive abilities. In the present study, we addressed these issues by analyzing the chronometry of intelligence-related differences in midfrontal global theta connectivity, which has been shown to reflect cognitive control functions. We demonstrate in a sample of 98 adults, who completed a cognitive control task while their electroencephalogram was recorded, that individual differences in midfrontal global theta connectivity during stages of higher-order information-processing explained 65% of the variance in fluid intelligence. In comparison, task-evoked theta connectivity during earlier stages of information processing was not related to fluid intelligence. These results suggest that more intelligent individuals benefit from an adaptive modulation of theta-band synchronization during the time-course of information processing. Moreover, they emphasize the role of interregional goal-directed information-processing for cognitive control processes in human intelligence and support theoretical accounts of intelligence, which propose that individual differences in cognitive control processes give rise to individual differences in cognitive abilities.

Keywords: chronometry, cognitive control, EEG, functional connectivity, intelligence

Individual differences in human intelligence determine the way individuals approach challenging problems in complex environments, how they develop strategies to adapt to their environments, and what they learn from experience (Neisser et al., 1996). Evidence for a considerable hereditary influence on human intelligence has been fueling the search for neural and cognitive endophenotypes, giving rise to individual differences in intelligence (Deary, Penke, & Johnson, 2010). A central role has been attrib-

uted to cognitive control processes—also referred to as executive attention, attentional control, executive control, inhibitory control, or executive functions—that act as an umbrella term for self-regulatory higher-order cognitive processes contributing to goal-directed behavior (Diamond, 2013). In a narrower sense, cognitive control processes are often defined as those processes that enable the transformation and manipulation of representations in working memory by activating goal-relevant information and/or inhibiting irrelevant information (Friedman & Miyake, 2017; Miyake & Friedman, 2012; Miyake et al., 2000; Smith & Jonides, 1999). Individual differences in cognitive control have been suggested to act as a domain-general bottleneck constraining performance in a variety of cognitive ability measures including but not limited to measures of fluid intelligence, working memory capacity, and processing speed (Engle, 2018; Kovacs & Conway, 2016, 2019).

There is a substantial body of research in cognitive psychology and cognitive neuroscience that supports the notion that individual differences in cognitive control are moderately to strongly related to individual differences in fluid intelligence.

The Role of Cognitive Control in Fluid Intelligence: Evidence From Cognitive Psychology

In cognitive psychology, individual differences in cognitive control are often measured as individual differences in the executive functions updating, shifting, and inhibition (Miyake et al.,

[ORCID] Anna-Lena Schubert, Dirk Hagemann, Christoph Löffler, and Jan Rummel, Institute of Psychology, Heidelberg University; Stefan Arnau, IfADo-Leibniz Research Centre for Working Environment and Human Factors, Dortmund, Germany.

Correspondence concerning this article should be addressed to Anna-Lena Schubert, Institute of Psychology, Heidelberg University, Hauptstrasse 47-51, D-69117 Heidelberg, Germany. E-mail: anna-lena.schubert@psychologie.uni-heidelberg.de

2000), with individual differences in updating (Friedman et al., 2006), updating and shifting (Friedman et al., 2008), or updating and inhibition (Wongupparaj, Kumari, & Morris, 2015) being substantially related to intelligence. Moreover, the common variance shared between all three executive functions has also been shown to be associated with intelligence beyond these function-specific associations (Friedman et al., 2006, 2008). Factor-analytical investigations based on the Cattell-Horn-Carroll model of cognitive abilities (CHC; Carroll, 1993) have shown that updating cannot be factor-analytically separated from the general memory factor g_m, whereas inhibition and shifting can be conceived of as a part or a narrow subfactor of the general speed factor g_s (Jewsbury, Bowden, & Strauss, 2016). In addition, Shipstead, Harrison, and Engle (2016) suggested that the ability to successfully disengage from irrelevant information held in working memory contributes to intelligence differences and may explain the substantial correlation between measures of working memory capacity and fluid intelligence (Ackerman, Beier, & Boyle, 2005; Kane, Hambrick, & Conway, 2005; Kyllonen & Christal, 1990; Oberauer, Schulze, Wilhelm, & Süss, 2005).

The Role of Cognitive Control in Fluid Intelligence: Evidence From Cognitive Neuroscience

Neuroscientific studies have consistently shown that an effective interaction between association cortices in frontal and parietal brain regions associated with higher-order cognitive control processes underlies individual differences in intelligence (Basten, Hilger, & Fiebach, 2015; Jung & Haier, 2007). Evidence for the relevance of parietal-frontal integration stems from numerous studies using various structural and functional neuroimaging techniques (Basten et al., 2015; Colom & Thompson, 2013) such as cortical surface area and cortical thickness analyses (Colom et al., 2013), voxel-based morphometry (Colom et al., 2013; Colom, Jung, & Haier, 2007), voxel-based lesion mapping (Gläscher et al., 2010), and functional MRI (fMRI; Burgess, Gray, Conway, & Braver, 2011). Moreover, electrophysiological studies using the event-related potential (ERP) technique have demonstrated that intelligent individuals showed processing advantages during very specific time windows, in which cognitive control processes take place (Schubert, Hagemann, & Frischkorn, 2017). In particular, more intelligent individuals showed substantially shorter P3 latencies, indicating that they benefited from a more efficient transmission of information from frontal attentional and working memory processes to temporal-parietal processes of memory storage.

Recent studies have gone beyond localizationist approaches and have emphasized the role of structural and functional interactions between brain networks for human intelligence. A network neuroscience perspective on human intelligence takes into account that the human brain is a complex network, which continuously processes, integrates, and updates information from functionally segregate interacting regions (Barbey, 2018; Sporns, 2011). Connectivity measures are often derived from fMRI and either describe white matter projections that link cortical regions (structural connectivity) or statistical patterns of dynamic interactions within and between cortical regions (functional connectivity), which have both been associated with intelligence (Booth et al., 2013; Cole, Yarkoni, Repovš, Anticevic, & Braver, 2012; Dubois, Galdi, Paul, & Adolphs, 2018; Ferrer et al., 2013; Hilger, Ekman, Fiebach, &

Basten, 2017a, 2017b; Kievit et al., 2016; Kocevar et al., 2019; Penke et al., 2012; Pineda-Pardo, Martínez, Román, & Colom, 2016; Tamnes et al., 2010; Wendelken et al., 2017; Wendelken, Ferrer, Whitaker, & Bunge, 2016).

Specifically, fractional anisotropy measures of white-matter tract integrity have been shown to be associated with intelligence and reasoning ability, across the whole brain (Ferrer et al., 2013; Penke et al., 2012) as well as within and between specific brain regions associated with higher-order attentional processes including the forceps minor, the corticospinal tract, the anterior thalamic radiation, the right superior longitudinal fasciculus, the uncinate fasciculus, the rostrolateral prefrontal cortex, and the inferior parietal lobe (Booth et al., 2013; Kievit et al., 2016; Pineda-Pardo et al., 2016; Tamnes et al., 2010; Wendelken et al., 2017). Moreover, individual differences in functional connectivity in and between certain frontoparietal brain networks that act as control regions or hubs and facilitate goal-directed information processing contribute to individual differences in intelligence (Cole et al., 2012; Hilger et al., 2017b; Wendelken et al., 2017). In one of the rare studies combining measures of structural and functional connectivity, Wendelken et al. (2017) demonstrated that frontoparietal white matter development is a prerequisite for frontoparietal functional connectivity and reasoning ability in adolescence. Most intriguingly, the effect of structural connectivity on fluid intelligence seems to be largely mediated by individual differences in processing speed and working memory (Ferrer et al., 2013; Fuhrmann et al., 2020; Kievit et al., 2016). This suggests that a greater integrity of frontoparietal white matter projections facilitates saltatory conduction across the axon and increases functional connectivity within and between brain regions associated with cognitive control, enhancing the speed and capacity of information-processing, which may translate into advantages in fluid intelligence.

Problems in the Measurement of Cognitive Control

Despite these promising results, there are some concerns regarding the measurement of individual differences in neurocognitive indicators of cognitive control that cast doubt on the conclusion that cognitive control plays a starring role in explaining intelligence differences.

Limitations of Behavioral Measures of Cognitive Control

There have recently been many concerns regarding cognitive control as a psychometric construct that challenge some of the previously discussed findings on the relation between behavioral measures of cognitive control and fluid intelligence (Frischkorn, Schubert, & Hagemann, 2019; Gärtner & Strobel, 2019; Hedge, Powell, & Sumner, 2018; Rey-Mermet, Gade, & Oberauer, 2018; Rey-Mermet, Gade, Souza, von Bastian, & Oberauer, 2019; Rouder & Haaf, 2019). To discuss the implications of these concerns, it is important to distinguish between studies that employ mean performance measures of cognitive control (i.e., performance in a specific condition or averaged across different conditions in an experimental task) and studies that employ difference score measures of cognitive control (i.e., difference scores or slope estimates between at least two experimental conditions). Both mean performance and difference score measures are typically

calculated based on the average number of correct responses and/or averaged response times (RTs) across experimental trials (Draheim, Mashburn, Martin, & Engle, 2019), but they can in principle also be calculated on the basis of other performance measures such as model-based estimates of information-processing (Frischkorn & Schubert, 2018; Hartmann, Rey-Mermet, & Gade, 2019).

Mean performance measures of cognitive control typically show high reliabilities but questionable validities. In particular, mean performance measures of RTs have been shown to largely reflect individual differences in general processing speed (Frischkorn et al., 2019). The large majority of studies reporting substantial correlations between cognitive control and fluid intelligence have predominantly employed mean performance measures (e.g., Chuderski, 2014; Redick et al., 2016; Unsworth, 2015; Unsworth, Redick, Lakey, & Young, 2010; Unsworth, Spillers, & Brewer, 2009; Wongupparaj et al., 2015). Because these mean performance measures are confounded with general processing capacities, these studies do not provide sufficiently compelling evidence for an association between cognitive control and fluid intelligence.

Difference score measures, on the other hand, are supposed to reflect individual differences in cognitive control more validly because they isolate the cognitive control process of interest by directly measuring interindividual differences in intraindividual experimental effects (but see Rey-Mermet et al., 2019; and Schubert, Hagemann, Voss, Schankin, & Bergmann, 2015 for criticisms of the underlying assumption of additive factors that experimental manipulations selectively affect a single process of interest). However, experimentally validated difference score measures of cognitive control are often task-specific, show low reliabilities, and show little variation between individuals (Gärtner & Strobel, 2019; Hedge et al., 2018; Rey-Mermet et al., 2018; Rouder & Haaf, 2019). For these reasons, correlations between difference score measures of cognitive control and fluid intelligence are typically lower than those of mean performance measures and often fail to reach statistical significance at all (e.g., Friedman et al., 2006; Frischkorn et al., 2019; Rey-Mermet et al., 2019).

Moreover, both mean performance and difference score measures of cognitive control are typically based on either correct response rates or RTs, which makes them prone to be affected by individual differences in speed–accuracy trade-offs (Draheim, Mashburn, et al., 2019; Rey-Mermet et al., 2019). This is particularly concerning for research on the elementary cognitive processes underlying intelligence, because more intelligent individuals adjust their decision criteria differently than less intelligent individuals to adapt to task demands (Draheim, Mashburn, et al., 2019; Schmiedek, Oberauer, Wilhelm, Süss, & Wittmann, 2007; Schubert, Hagemann, Löffler, & Frischkorn, 2020). In theory, more intelligent individuals should benefit from more efficient cognitive control processes, resulting in faster and more accurate responses in cognitive control tasks (i.e., higher mean performance) and a smaller impairment in performance by experimentally induced increased control demands (i.e., smaller difference scores). However, because they typically have more liberal decision criteria than less intelligent individuals, they may show even faster RTs at the cost of decreases in accuracy rates. Moreover, experimentally induced increases in cognitive control demands may further moderate this interaction in unexpected ways, further complicating the interpretation of associations between measures of intelligence and cognitive control.

Taken together, these limitations call into question whether cognitive control can be reliably and validly measured using accuracy rates and mean RTs in experimental tasks. Various solutions for improving the measurement of cognitive control have been suggested, including hierarchical modeling (Rouder & Haaf, 2019), the use of mathematical models (Frischkorn & Schubert, 2018), the introduction of individually calibrated response deadlines (Rey-Mermet et al., 2019), and the development of new experimental tasks (Draheim, Tsukahara, Martin, Mashburn, & Engle, 2019). Undoubtedly, these promising approaches will allow a better evaluation of cognitive control as a psychometric construct and refine our understanding of the role of cognitive control processes in intelligence. As it stands, however, it is difficult to evaluate the role of cognitive control processes measured on a behavioral level—either as mean performance or difference scores—in intelligence due to the measurement problems mentioned above.

Limitations of Neural Correlates of Cognitive Control

In comparison, neural correlates of cognitive control have recently seen a huge rise in popularity in individual differences research. In particular, network neuroscience measures of cognitive control hubs have become increasingly popular in intelligence research (e.g., Barbey, 2018; Cole et al., 2012; Hilger et al., 2017a, 2017b; Wendelken et al., 2017) and correlations between measures of frontoparietal functional connectivity and intelligence have been interpreted as evidence for the role of cognitive control in intelligence. However, if individual differences in frontoparietal functional connectivity underlie individual differences in cognitive control, and if cognitive control plays a central role in intelligence differences, it may seem surprising that measures of functional connectivity rarely explained more than 20% of variance in cognitive abilities in any of these studies (e.g., Song et al., 2008). There are three shortcomings of previous studies that may have led to an underestimation of the association between functional cognitive control network characteristics and intelligence.

Up to now, the majority of studies on the functional network dynamics underlying intelligence have used resting-state fMRI data, which has two limitations. First, resting-state data do not inform us about dynamic network interactions during cognitive control processes such as the task-evoked elicitation of network dynamics and the suppression of ongoing activity in task-irrelevant areas (He, 2013). Functional connectivity measures reflecting such task-related network reconfigurations and activations during cognitive control processes may therefore show greater correlations with intelligence than functional connectivity measures derived from resting-state data. Second, measures with a slow sampling rate such as the fMRI are not well-suited to account for the temporal dynamics of functional connectivity (Sporns, 2013).

These two shortcomings may pose a problem, because previous research on the neural correlates of intelligence using the electroencephalogram (EEG) revealed that more intelligent individuals showed processing advantages only during specific time windows associated with higher-order control processes (Schubert et al., 2017). In particular, only the latencies of ERP components associated with higher-order cognitive processes occurring later in the

stream of processing and specifically the latencies of the P3 component were negatively associated with intelligence. These results indicate that associations between neural processing correlates and cognitive abilities fluctuate over time and may be largest when information is processed in working memory and subsequently transmitted from frontal control and working memory processes to temporal-parietal processes of memory storage (Polich, 2007). If dynamic interactions within and between cortical regions underlying these cognitive processes give rise to the association between functional connectivity measures and intelligence, it should be greatest specifically while individuals engage in higher-order cognitive processes. Therefore, previous studies may have underestimated this association, because the comparatively low temporal resolution of fMRI does not allow to capture fluctuations in functional connectivity during such short periods of time and because the data were collected during resting-state.

Moreover, a higher temporal resolution of functional connectivity measures would allow investigating whether individual differences in functional connectivity during higher-order information processing explain the association between the P3 latencies and intelligence. This would be particularly illuminating regarding causal mechanisms underlying the association between neural processing speed and intelligence, as attempts to pharmacologically enhance neural processing speed did not translate into better performance in intelligence tests (Schubert, Hagemann, Frischkorn, & Herpertz, 2018). This lack of transfer suggests that structural or functional brain properties may act as confounding variables in the way that advantages in those brain properties may enhance both the speed of information processing and intelligence.

The Present Study

The aim of the present study was to address these issues by analyzing the chronometry of intelligence-related differences in task-evoked functional connectivity. For this purpose, we calculated the connectivity degree at a midfrontal electrode evoked in a cognitive control task and used structural equation models to decompose the time-course of functional connectivity correlations with intelligence. Phase-synchronized oscillatory activity is a prime candidate for the facilitation of interregional goal-directed information processing associated with cognitive control processes (Cole et al., 2012; Hilger et al., 2017b; Pineda-Pardo et al., 2016; Wendelken et al., 2017), because it coordinates interregional communication and information-transfer in specific time windows (Fries, 2005). In particular, synchronized oscillatory activity in the theta-band has been suggested to underlie the functional networks associated with the P3 (Harper, Malone, & Iacono, 2017), with the medial frontal cortex acting as a central hub for long-range information transmission (Cohen, 2011; Helfrich & Knight, 2016). The connectivity degree as a measure of relative functional connectivity reflects the extent to which an area acts as a global hub in information-processing, with greater connectivity degrees indicating greater centrality (greater "hubbiness") of a node in goal-directed information-processing.

If more intelligent individuals benefited from a more efficient neural organization of long-range information transmission during higher-order processing, they should show an overall stronger theta connectivity at frontal midline electrodes during stages of information-processing associated with cognitive control pro-

cesses. Hence, we predict that individual differences in midfrontal global theta connectivity will be associated with individual differences in intelligence. This should be the case particularly during later stages of higher-order information processing linked to the P3 time window, but not (or less strongly) during earlier stages of sensory information processing. Moreover, we expect individual differences in connectivity degrees during the P3 time window to explain the association between P3 latencies and intelligence by accounting for the functional network dynamics giving rise to the association between neural processing speed and intelligence.

Method

Participants

We recruited a sample of $N = 100$ participants between 18 and 60 years old from different educational and occupational backgrounds via local newspaper advertisement, announcements on social media platforms, and distribution of flyers in Heidelberg. Because two participants did not complete the experiment, the final sample consisted of $N = 98$ participants (64 females, 34 males) with a mean age of $M = 31.9$ ($SD = 13.3$). Following recommendations by Browne and Cudeck (1992), sample size was determined based on the hypothesis of close fit (H0: $\varepsilon \leq .05$, H1: $\varepsilon \geq .10$) for the structural equation model with the fewest degrees of freedom ($df = 63$), an alpha error of $\alpha = .05$, and a power of $1 - \beta = .80$. The resulting minimum sample size was $N = 83$. We recruited more participants to increase power and the stability of parameter estimates.

All participants had normal or corrected to normal vision and no mental illness. Participants signed an informed consent form prior to their participation. They received 30€ and feedback about their intelligence test results as reward for their participation. The study was approved by the ethics committee of the faculty of behavioral and cultural studies, Heidelberg University. All procedures were conducted in accordance with the declaration of Helsinki.

Materials

Cognitive control task. We used a shifting task (Sudevan & Taylor, 1987) to measure participants' performance in an attention control task because previous research demonstrated that switch in comparison to repeat trials in this task evoked significantly stronger long-range theta coupling between prefrontal and posterior brain regions, reflecting top-down activation and transfer of information between memory systems (Sauseng et al., 2006). Moreover, its relatively low perceptual demands and perceptual constancy across experimental conditions make it highly suitable for task-related EEG recording as demonstrated in previous studies (Frischkorn et al., 2019; Sauseng et al., 2006).

Participants were presented with single-digit numbers between 1 and 9 (the number 5 was excluded) and had to decide for each number whether it was less or more than 5 (less/more condition) or whether it was odd or even (odd/even condition) by pressing one of two keys with their index fingers. Which of these two decision rules participants had to follow changed across trials and was indicated by the coloring of the number. Participants completed 40 practice trials with feedback and 640 experimental trials in 10 blocks without feedback. Of these 640 trials, 50% belonged to the

less/more condition and 50% belonged to the odd/even condition, respectively. In addition, in 50% of the trials participants had to shift their task set with regard to the previous trial (shifting condition), whereas in the other 50% of the trials they followed the same decision rule as in the previous trial (repeat condition).

Each trial began with a gray fixation cross shown on a black screen for 512–768 ms, followed by a blank screen presented for 1,024–1,278 ms. Next, a colored digit appeared on a black screen at a visual angle of 0.60° and remained there for 1,024–1,278 ms after participants had responded, followed by an intertrial interval that consisted of a black screen and lasted 1,000–1,500 ms. On a small number of randomly determined trials, participants saw thought probes following their response, which asked them to indicate where they had just been with their thoughts (data not reported here).

Berlin intelligence structure test (BIS). We administered the short version of the Berlin intelligence structure test (Jäger, Süß, & Beauducel, 1997) to measure fluid intelligence. The BIS is based on the bimodal Berlin intelligence structure model, which distinguishes between four operation-related (processing speed, memory, creativity, processing capacity) and three content-related (verbal, numerical, figural) components of intelligence. The test consists of 15 tasks, with each task being a combination of one operation-related component with one content-related component of intelligence. Following the test manual, participants' scores for the four process-related components were computed by aggregating the normalized scores of all tasks related to the respective operation and content components. These process-related component scores were then transformed into z-scores for further analyses. One participant's processing speed score was removed from further analyses because it exceeded ±3 SDs of the sample mean. Participants had a mean IQ score of $M = 95.32$ ($SD = 12.08$). This is likely an underestimation of their true intelligence, as the BIS only contains norm data for senior high school students between 16 and 19 years. The mean score of the processing speed component in this sample was $M = 100.26$ ($SD = 8.48$), the mean score of the memory component was $M = 97.70$ ($SD = 7.84$), the mean score of the creativity component was $M = 97.62$ ($SD = 7.06$), and the mean score of the processing capacity component was $M = 100.04$ ($SD = 8.28$).

Procedure

We first administered the BIS, followed by the cognitive control task, two working memory tasks, a metronome response task, a mind-wandering questionnaire, and a questionnaire about demographic data. Data from the working memory tasks, metronome response task, and mind-wandering questionnaire are not reported in the present paper. During the cognitive control task, participants sat in a dimly lit, sound-attenuated cabin while their EEG was recorded. Each session took about 3.5 hr.

EEG Recording

The EEG was recorded with 32 equidistant Ag/AgCl electrodes (32Ch-EasyCap, EASYCAP, Herrsching, Germany) and amplified by a BrainAmp DC amplifier (Brain Products, Gilching, Germany). We used the aFz electrode as the ground electrode. Electrodes were initially referenced to Cz and offline rereferenced to an average reference. All electrode impedances were kept below 5 kΩ. The EEG signal was recorded continuously with a sampling rate of 1024 Hz (high-pass 0.1 Hz). EEG data from one participant were lost because of technical failure.

Data Analysis

Behavioral data. We only analyzed RTs in trials with correct responses. RTs faster than 100 ms or slower than 3,000 ms, or with logarithmized RTs exceeding ±3 SDs of the mean of each condition, were discarded. Mean RTs were calculated separately for each experimental condition. Across all experimental conditions, less than one percent of mean RTs exceeded ±3 SDs of their respective condition mean and were excluded as outliers.

Electrophysiological data. EEG data were preprocessed with the open source toolbox EEGLAB (Delorme & Makeig, 2004) with MATLAB (The MathWorks Inc., Natick, Massachusetts). Bad channels were identified and subsequently removed based on probability, kurtosis, and spectrum of the channel data. Epochs were 5,000 ms long and began 2,500 ms before stimulus onset. We conducted independent component analyses (ICA) with data down-sampled to 200 Hz to identify and remove ocular artifacts and generic discontinuities based on visual inspection and the ADJUST algorithm (Mognon, Jovicich, Bruzzone, & Buiatti, 2011). Subsequently, artifact-containing segments were automatically detected and rejected with 1,000 μV as the threshold for detecting large fluctuations, 5 SDs as the probability threshold for the detection of improbable data, and 5% as the maximum number of epochs to be rejected per iteration.

Neural processing speed. Consistent with previous studies from our lab (Schubert et al., 2015, 2017; Schubert, Hagemann, Löffler, & Frischkorn, 2020; Schubert, Nunez, Hagemann, & Vandekerckhove, 2018), the data were filtered offline with a low-pass filter of 16 Hz to allow the identification of individual P3 peak latencies. The peak latency reflects the time-to-peak for an ERP component and indicates the time at which the amplitude of a component reaches its maximum. P3 latencies were determined at the parietal electrode over midline separately for each experimental condition and subsequently z-standardized for further analyses. We chose this electrode for peak detection because the P3 is typically recorded at parietal electrode sites (Verleger, 2020) and because this facilitated consistency and comparability to previous studies (Schubert et al., 2017, 2015; Schubert, Hagemann, et al., 2018). Across all experimental conditions, less than one percent of P3 latency values exceeded ±3 SDs of their respective condition mean and were excluded as outliers. Two participants did not show a visually identifiable P3 component; hence, no P3 peak latencies were determined for those two participants.

Functional connectivity. Prior to the time-frequency analyses, the data were filtered offline with a low-pass filter of 25 Hz. Time-frequency decomposition was performed by convolving stimulus-locked data from all electrodes with complex Morlet wavelets with frequencies ranging from 1 to 20 Hz in 20 logarithmically spaced steps. The number of cycles n used to specify the width of the Gaussian distribution was set to 4 to provide a good trade-off between temporal and frequency resolution. Frequency-specific phases at each time point t were defined as arctan(real$[Z_t]^2$/imag$[Z_t]^2$) of the complex convolution signal Z. As a measure of functional connectivity in the theta range, the phase lag

index (PLI; Stam, Nolte, & Daffertshofer, 2007) was calculated for the frequency of 6 Hz. The PLI quantifies the extent to which a distribution of phase angle differences is tilted toward positive or negative sides of the imaginary axis. The distribution is expected to be symmetric if there is no coupling, resulting in a PLI of zero, whereas the PLI is one if all imaginary parts of the phase angle difference estimates at a given time-frequency point are either positive or negative. Calculating connectivity measures based on the PLI ensures that individual differences in phase synchronization do not simply reflect individual differences in volume conduction, as the PLI is insensitive to volume conduction: A common source (such as volume conduction) being reflected in multiple time series would result in phase angle differences of zero, which is a value that is ignored by the PLI. Other data-analytic procedures such as combining imaginary coherence approaches with source modeling can further ameliorate this issue (Haufe, Nikulin, Müller, & Nolte, 2013), but were not applicable in the present study due to the low spatial sampling density of our electrode montage.

We subsequently calculated the connectivity degree (CD) as a graph theoretic connectivity measure of global functional connectivity, which indicates the degree to which an electrode area acts as a hub in the brain's network (Cohen, 2014). Connectivity degrees were calculated based on the binarized interchannel connectivity matrices by summing the number of suprathreshold connections at each sampling point separately for each electrode and each of the four experimental conditions. We binarized the connectivity matrices using a threshold of the median PLI plus 1 standard deviation at each individual time point. A high CD value indicates that an electrode has many suprathreshold interchannel connections at a certain sampling point, whereas a low CD value conversely indicates that an electrode has only a limited number of suprathreshold interchannel connections at a certain sampling point. All statistical analyses are based on CD values at a frontal electrode slightly anterior of Fz. For exploratory analyses, these frontal CD values at each sampling point were entered into structural equation models to illustrate the time-course of correlations between functional connectivity and intelligence. For confirmatory analyses, frontal CD values were averaged separately for two time windows reflecting earlier and later stages of information processing, respectively. The time window reflecting later stages of higher-order information processing was determined as a symmetric time window of ± 1.5 SD around the average P3 latency across all experimental conditions and ranged from 335 to 575 ms after stimulus onset. The complementary earlier time window ranged from 0 to 335 ms after stimulus onset. Connectivity measures were averaged separately for each of the two time windows and the four experimental conditions. Subsequently, all values were z-standardized for further analyses. Across both time windows and all experimental conditions, one percent of connectivity degree values exceeded ± 3 SDs of their respective condition mean and were excluded as outliers.

Statistical Analyses

Structural equation modeling. We used structural equation models to assess the associations between functional connectivity measures, general intelligence, and processing speed. We entered condition-specific measures of functional connectivity and pro-

cessing speed and operation-specific intelligence test scores as indicators into these analyses (see Figure 1 for details regarding the data entered into structural equation models). All models were fitted with the R package *lavaan* (Rosseel, 2012) with the maximum likelihood algorithm with robust Huber-White standard errors and a scaled test statistic equal to the Yuan-Bentler test statistic to account for the nonnormality of some connectivity measures and possible deviations from multivariate normality.

We evaluated goodness-of-fit based on the comparative fit index (CFI; Bentler, 1990) and the root mean square error of approximation (RMSEA; Browne & Cudeck, 1992) and compared model fit of any two models with the likelihood ratio test. Following the recommendations by Browne and Cudeck (1992) and Hu and Bentler (1999), we considered CFI values > .90 and RMSEA values < .08 to indicate acceptable model fit, and CFI values > .95 and RMSEA values < .06 to indicate good model fit. The statistical significance of model parameters was assessed with the two-sided critical ratio test.

Cluster-based permutation tests. To test for significant correlations between fluid intelligence and connectivity degrees in Time $\times$ Sensor space, we performed a cluster-based permutation test (Maris & Oostenveld, 2007) using FieldTrip (Oostenveld, Fries, Maris, & Schoffelen, 2011). This approach controls for Type I error rates, which is crucial when performing multiple comparisons. We entered measures of functional connectivity averaged across the four experimental conditions and intelligence test scores averaged across the four subscales into these analyses to increase their reliability (see Figure 1 for details regarding the data entered into structural equation models). Because the connectivity degree measure was calculated based on the PLI (Stam et al., 2007) and the PLI is based on binarizing phase angles, both measures exhibit high frequency fluctuations in the time domain. To identify coherent clusters of significant correlations over time, we applied temporal smoothing to the connectivity degree time series, using a moving average window with a width of 50 data points. A clustering algorithm identified clusters of neighboring data points in Time $\times$ Sensor space which represented correlations associated with $p < .05$. The test statistic for each cluster consisted of the summed t values of the data points of the respective cluster. The way the cluster-based permutation approach controls for Type I errors, is by comparing the cluster test statistics against a (H0-) distribution of maximum test statistics obtained by computing the test-statistics on permuted data in a certain number of iterations, in this case 1,000 iterations. Finally, the observed test statistics were compared to the H0-distribution in a one-sided test. Clusters with $p < .05$ were regarded as significant.

Data and code availability. The data supporting the findings of the study and the statistical analysis code used in the article are available in the Open Science Framework repository at https://osf .io/vtzaq/ (Schubert, Hagemann, Löffler, Rummel, & Arnau, 2020).

Results

We used structural equation models to assess the associations between connectivity degree as a measure of global functional connectivity in the theta-band, general intelligence, and processing speed. Mean connectivity degrees, RTs, and P3 latencies are

	Experimental task and behavioral data	Intelligence testing and intelligence test data	EEG recording and EEG data
Procedure	■ Shifting task (Sudevan & Taylor, 1987) 　■ 2 Task (less/more vs. odd/even) x 2 Shifting (shifting vs. repeat) within-subject design 　■ 640 trials (160 trials per cell)	■ Berlin Intelligence Structure Test (Jäger et al., 1997) 　■ 4 operation-related components (processing speed, memory, creativity, processing capacity) 　■ 3 content-related components (verbal, numerical, figural) 　■ 15 tasks	■ 32 Ag/AgCl electrodes ■ Ground: aFz ■ Reference: Cz ■ Sampling rate: 1024 Hz ■ 0.1 Hz high-pass filter
Data preprocessing and analysis	■ Discarding of trials 　■ incorrect trials 　■ RT < 150 ms 　■ RT > 3000 ms 　■ logRT > ± 3 SDs of each condition mean ■ Calculation and z-standardization of mean RTs per condition ■ removal of outlier values (< 1 %)	■ Calculation and z-standardization of the four operation-related component scores according to the manual ■ removal of outlier values (< 1 %)	■ Identification of bad channels ■ Epoching (2500 ms before to 2500 ms after stimulus onset) ■ Artifact removal with ICA and ADJUST (Mognon et al., 2011) ■ Subsequent automatic artifact rejection ■ P3 latencies 　■ 16 Hz low-pass filter 　■ latencies were determined separately for each condition at a parietal electrode over midline 　■ z-standardization 　■ removal of outlier values (< 1 %) ■ Connectivity degrees (CDs) 　■ 25 Hz low-pass filter 　■ time-frequency decomposition with frequencies from 1 to 20 Hz in 20 logarithmically spaced steps and 4 cycles 　■ calculation of phase lag index 　■ binarization of inter-channel connectivity matrices 　■ calculation of CDs by summing the number of superthreshold connections 　■ averaging and z-standardization of CDs over earlier (0 - 335 ms) and later (335 - 575 ms) time window 　■ removal of outlier values (1 %)
SEM	■ condition-specific mean RTs were entered as indicator variables	■ operation-related component scores were entered as indicator variables	■ condition-specific P3 latencies were entered as indicator variables ■ condition- and time-window-specific CD values were entered as indicator variables
Permutation tests	■ analyses did not include mean RTs	■ a general fluid intelligence variable was calculated by averaging across operation-related component scores	■ analyses did not include P3 latencies ■ a general CD variable was calculated by averaging across conditions

Figure 1. Design schematic of the data collection procedure and data analyses. EEG = electroencephalogram; RT = response time; logRT = logarithmized RT; ICA = independent component analysis; SEM = structural equation model.

Table 1

Mean (SD in Parentheses) Connectivity Degrees for the Earlier Time Window (0–335 ms After Stimulus Onset; N = 97), Connectivity Degrees for the Later Time Window (335–575 ms After Stimulus Onset; N = 97), Reaction Times (in ms; N = 98), and P3 Latencies (in ms; N = 95)

Measure	Connectivity degree (earlier time window)	Connectivity degree (later time window)	Reaction time	P3 latency
Odd/Even – repeat	6.40 (1.37)	6.86 (1.31)	916.20 (190.88)	456.82 (81.53)
Odd/Even – switch	6.14 (1.46)	6.70 (1.58)	1000.71 (224.27)	452.42 (90.27)
Less/More – repeat	6.26 (1.46)	6.60 (1.45)	873.90 (155.81)	456.89 (82.58)
Less/More – switch	6.12 (1.43)	6.71 (1.38)	942.97 (194.11)	451.76 (79.75)

Note. Odd/Even – repeat = repeat trials in the odd/even condition; Odd/Even – switch = switch trials in the odd/even condition; Less/More – repeat = repeat trials in the less/more condition; Less/More – switch = switch trials in the less/more condition.

shown in Table 1 for each of the four conditions in the cognitive control task. The full correlation matrix is shown in Figure 2.

Figure 3 displays a graphical representation of our main results that we will first describe and subsequently test. Consistent with our hypotheses, more intelligent individuals showed greater connectivity degrees during later stages, but not during earlier stages of information processing (see Figure 3). In particular, both a comparison between more and less intelligent individuals (Figure 3A) and an inspection of the estimated latent correlations (Figure 3B) across all sampling points indicated that more intelligent participants showed higher connectivity degrees during later stages of information-processing, in particular in a time window between 400 – 700 ms after stimulus onset. This positive association between connectivity degrees and intelligence test scores during later stages of processing was greatest at frontal electrodes and reversed at parieto-occipital electrodes (see Figure 3C, which shows the correlations between connectivity degree and fluid intelligence at each electrode).

These findings were corroborated by results from four structural equations models that explored the associations between functional connectivity and fluid intelligence (*gf*) during earlier and later stages of information processing. The models shown in Figure 4A–4C tested whether functional connectivity during all or during particular stages of information processing correlated with fluid intelligence. Although the models shown in Figure 4A–4C are mathematically equivalent, they were nevertheless all specified to provide different perspectives on and to evaluate the robustness of the relationship between fluid intelligence and functional connectivity. Due to their mathematical equivalence, they accounted for the data equally well, as reflected in identical fit statistics. The models provided an excellent account of the data, $\chi^2(63) = 56.20$, $p = .715$, CFI = 1.00, RMSEA = 0.00 (95% CI [0.00, 0.05]). Across all three models, we found converging evidence that the variance specific to functional connectivity during later stages of information-processing was substantially related to fluid intelligence, whereas functional connectivity during earlier stages of information-processing and overall functional connectivity across the whole time-course of information processing (captured in the hierarchical latent variable) were not related to fluid intelligence. The latter two were only spuriously related to fluid intelligence when the model did not include an association between functional connectivity during later stages of information-processing and fluid intelligence (see Figure 4C). These spurious correlations disappeared when the latent factor specific to functional connec-

tivity during later stages of information-processing was allowed to directly correlate with fluid intelligence (see Figure 4A and 4B), because it then did not have to exert its influence on fluid intelligence via the hierarchical latent variable.

Because structural equation models did not allow to relate all three variables (overall functional connectivity, functional connectivity during earlier stages of information-processing, functional connectivity during later stages of information-processing) to fluid intelligence simultaneously owing to reasons of submodel identifiability and multicollinearity, we specified two separate structural equation models describing (a) individual differences in functional connectivity and (b) individual differences in fluid intelligence to extract individual estimates of the latent variables for each participant. Subsequently, we correlated the estimates of all three latent functional connectivity variables (i.e., the latent functional connectivity variable across both time windows and the residuals of functional connectivity in the earlier and later time windows) with the latent intelligence variable using Pearson correlations. This analysis has the advantage of allowing the simultaneous estimation of correlations of all three functional connectivity variables with fluid intelligence. However, it comes with a caveat: Because correlations are only estimated at the manifest level, treating latent parameter estimates as observed variables violates mathematical assumptions by ignoring estimation uncertainty. This leads to an underestimation of standard errors and an overestimation of statistical significance of the estimated correlations. Nevertheless, we conducted this analysis to supplement conclusions from the formally more rigid structural equation models presented above.

Both the higher-order functional connectivity variable and the variable specific to functional connectivity in the later time-window were related to intelligence, $r = .23$, $p = .025$, and $r = .34$, $p < .001$, respectively, whereas functional connectivity in the earlier time-window was unrelated to intelligence, $r = .08$, $p = .424$. All three correlations differed significantly from each other, $p \leq .002$, suggesting that the correlation between fluid intelligence and functional connectivity in the later time window was larger than the correlation between fluid intelligence and functional connectivity across both time windows, which was in turn larger than the correlation between fluid intelligence and functional connectivity in the earlier time window.

Subsequently, we tested a fourth model that allowed a correlation between functional connectivity during later stages of information processing and intelligence only, with all other correlations between functional connectivity measures and intelligence fixed to
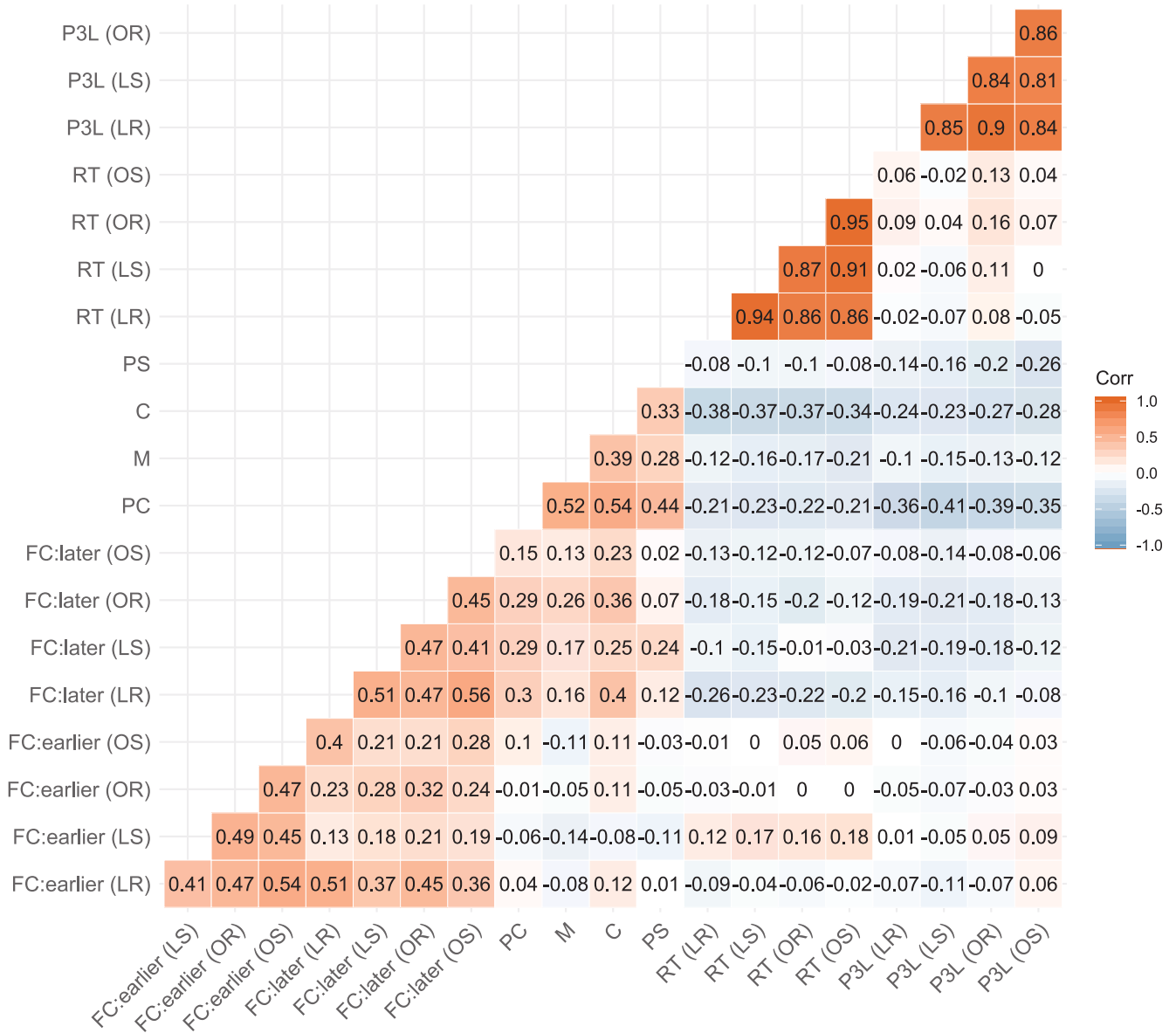
Figure 2. Pearson correlations between connectivity measures ($N = 97$), intelligence test scores ($N = 98$), reaction times ($N = 98$) and P3 latencies ($N = 95$). FC:earlier = functional connectivity during earlier stages of information processing (0–335 ms after stimulus onset); FC:later = functional connectivity during later stages of information processing (335–575 ms after stimulus onset); RT: reaction times; P3L: P3 latency; OR = odd/even task repeat condition; OS = odd/even task shift condition; LR = less/more task repeat condition; LS = less/more task shift condition; PC = processing capacity; PS = processing speed; M = memory; C = creativity. See the online article for the color version of this figure.

zero (see Figure 4D). These modifications did not lead to a deterioration of model fit, $\chi^2(64) = 56.19$, $p = .746$, CFI = 1.00, RMSEA = 0.00 (95% CI [0.00, 0.05]), $\chi^2_{LLR}(1) = 0.02$, $p = .890$. Functional connectivity in the theta-band during later stages of information processing was positively related to fluid intelligence, $r = .81$, $p < .001$, 95% CI [.43, 1.00], and explained 65.12% of variance in general intelligence (see Figure 5D).

Finally, we tested whether model comparisons supported the conclusion that individual differences in functional connectivity were related to fluid intelligence only during later, but not during earlier stages of information processing. For this purpose, we specified two additional models, which were modifications of the model shown in Figure 4A. In the first model, we imposed equal residual variances on the latent factors of functional connectivity during earlier and later stages of information processing and allowed both latent factors to correlate freely with fluid intelligence. This model still provided an adequate account of the data, $\chi^2(64) = 56.38$, $p = .740$, CFI = 1.00, RMSEA = 0.00
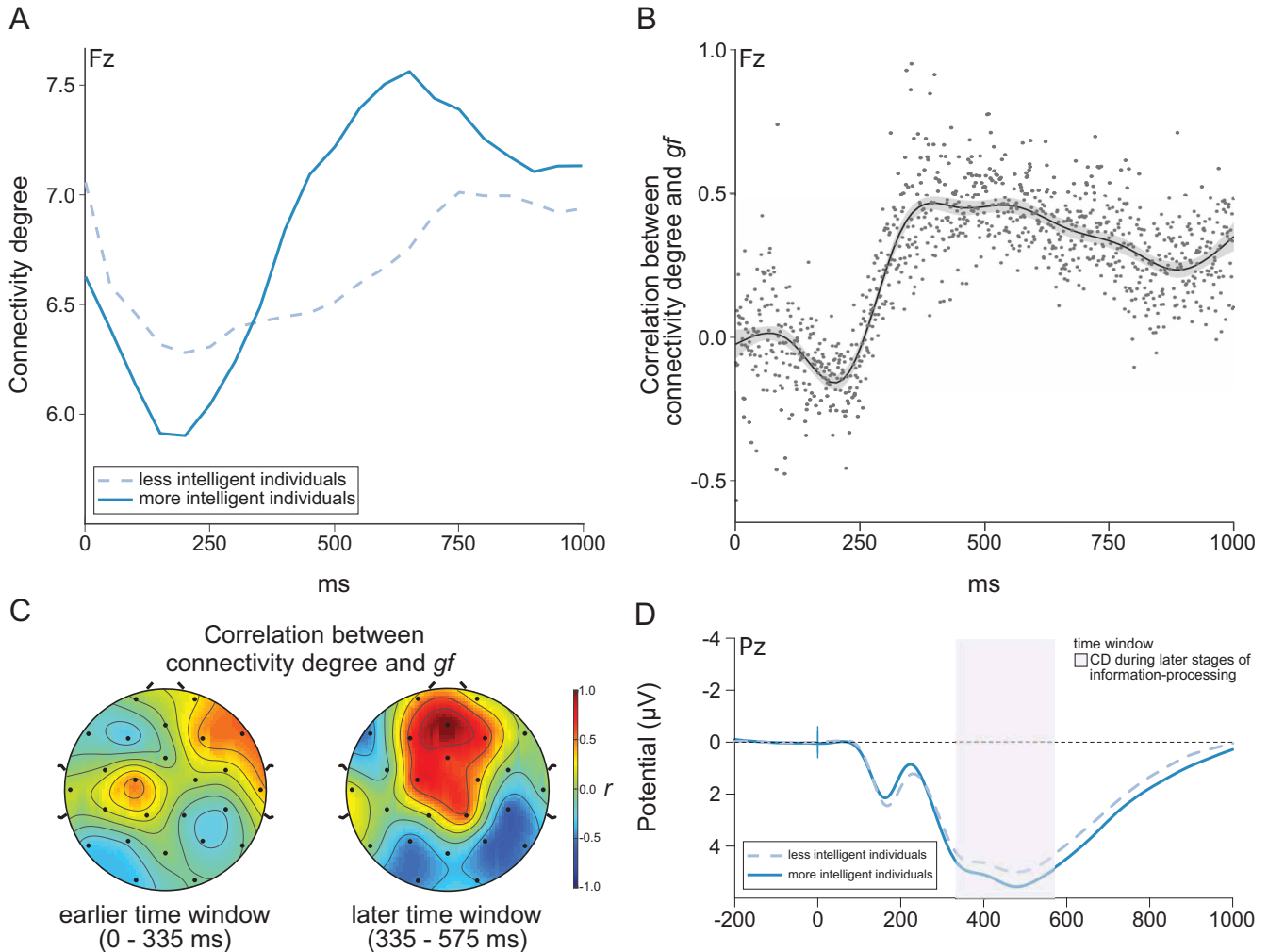
Figure 3. Descriptive overview of associations between connectivity degree and P3 latencies with intelligence test scores. All data were averaged across experimental conditions. (A) Differences in connectivity degree between more and less intelligent participants. Groups were allocated based on a median split of their mean scores on the four intelligence subtests. This median split was introduced to illustrate the time-course of group differences; all statistical analyses were conducted with the continuous intelligence test scores. $N = 97$. (B) Latent correlations between connectivity degree and fluid intelligence (gf) across all sampling points. Each of the 1,000 dots represents a single latent correlation estimated via structural equation modeling at the respective sampling point. $N = 98$. (C) Topography of latent correlations between fluid intelligence (gf) and average connectivity degree during the earlier (0–335 ms) and later (335–575 ms) time window depending on the location of the seed electrode. $N = 98$. (D) Differences in the grand average of the event-related potential measured at Pz between more and less intelligent participants. The shaded area indicates the time window of ± 1.5 SD around the average P3 latency, which was used to calculate the average connectivity during later stages of information-processing. $N = 95$. See the online article for the color version of this figure.

(95% CI [0.00, 0.05]), and model fit did not deteriorate significantly in comparison to the model without equal residual variances shown in Figure 4A, $\chi^2_{LLR}(1) = 0.00$, $p = .953$. We then specified a second model in which we forced both factors to covary equally with fluid intelligence, which deteriorated model fit significantly in comparison to the model without this restriction, $\chi^2(65) = 71.69$, $p = .266$, CFI $= .98$, RMSEA $= 0.03$ (95% CI [0.00, 0.07]), $\chi^2_{LLR}(1) = 27.36$, $p < .001$, which suggests that the associations of connectivity degrees with fluid intelligence differed significantly across earlier and later stages

of information processing. Taken together, this confirms our conclusion that individual differences in functional connectivity were related to fluid intelligence only during later, but not during earlier, stages of information processing.

Are These Results Confirmed by More Data-Driven Analyses?

In cognitive neuroscience, there are, broadly speaking, two approaches to data analysis. One approach is to define a priori
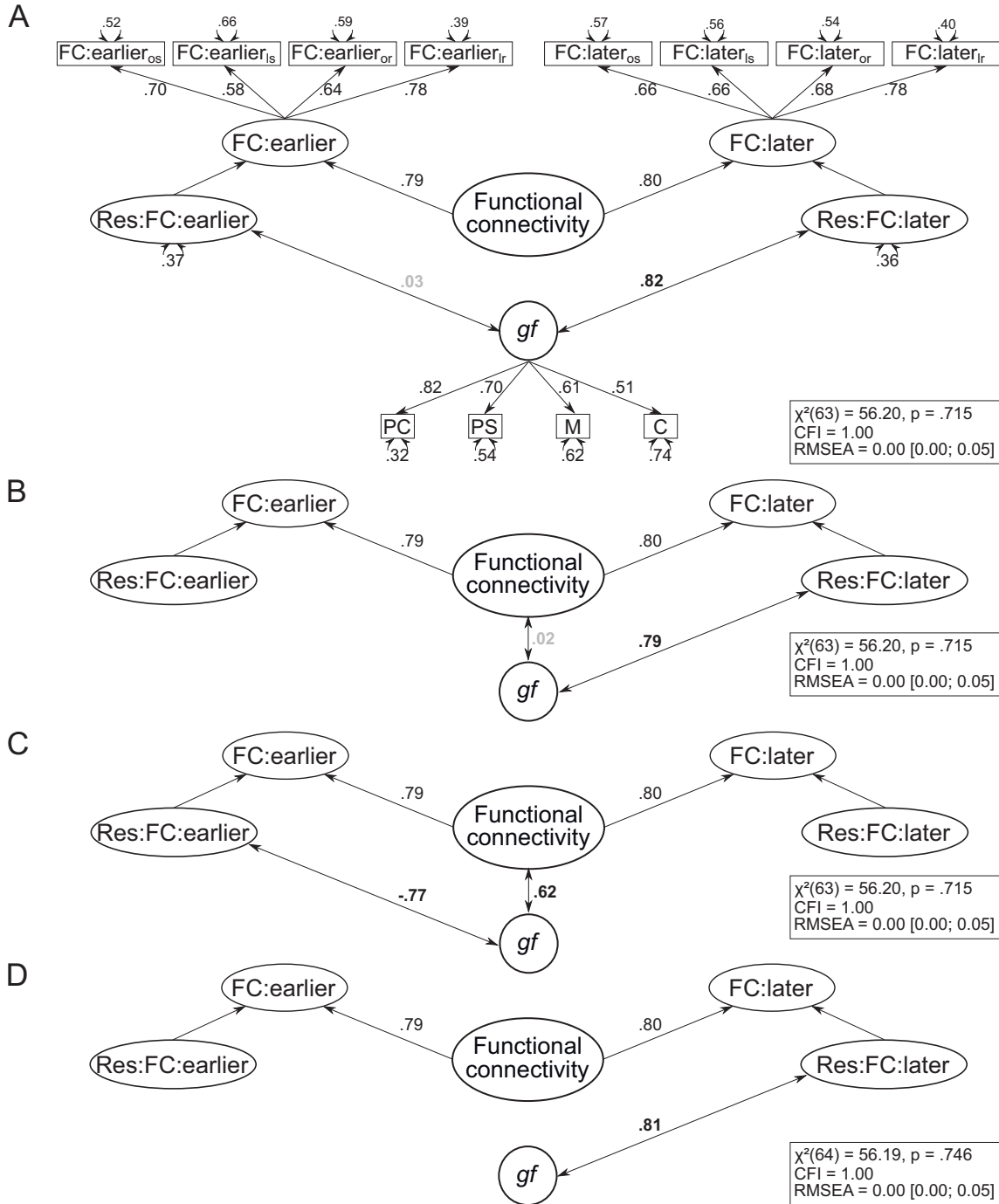
Figure 4. Graphical illustration of four structural equation models on the association between functional connectivity and fluid intelligence during earlier and later stages of information processing. Standardized regression weights and correlation coefficients are shown next to paths. Nonsignificant correlations are grayed out. Because of their mathematical identity, identical fit statistics are reported for the models shown in A, B, and C. FC:earlier = functional connectivity during earlier stages of information processing (0–335 ms after stimulus onset); FC:later = functional connectivity during later stages of information processing (335–575 ms seconds after stimulus onset); Res:FC:earlier = residual of the latent FC:earlier variable; Res:FC:later = residual of the latent FC:later variable; *gf* = fluid intelligence; or = odd/even task repeat condition; os = odd/even task shift condition; lr = less/more task repeat condition; ls = less/more task shift condition; PC = processing capacity; PS = processing speed; M = memory; C = creativity. *N* = 98.
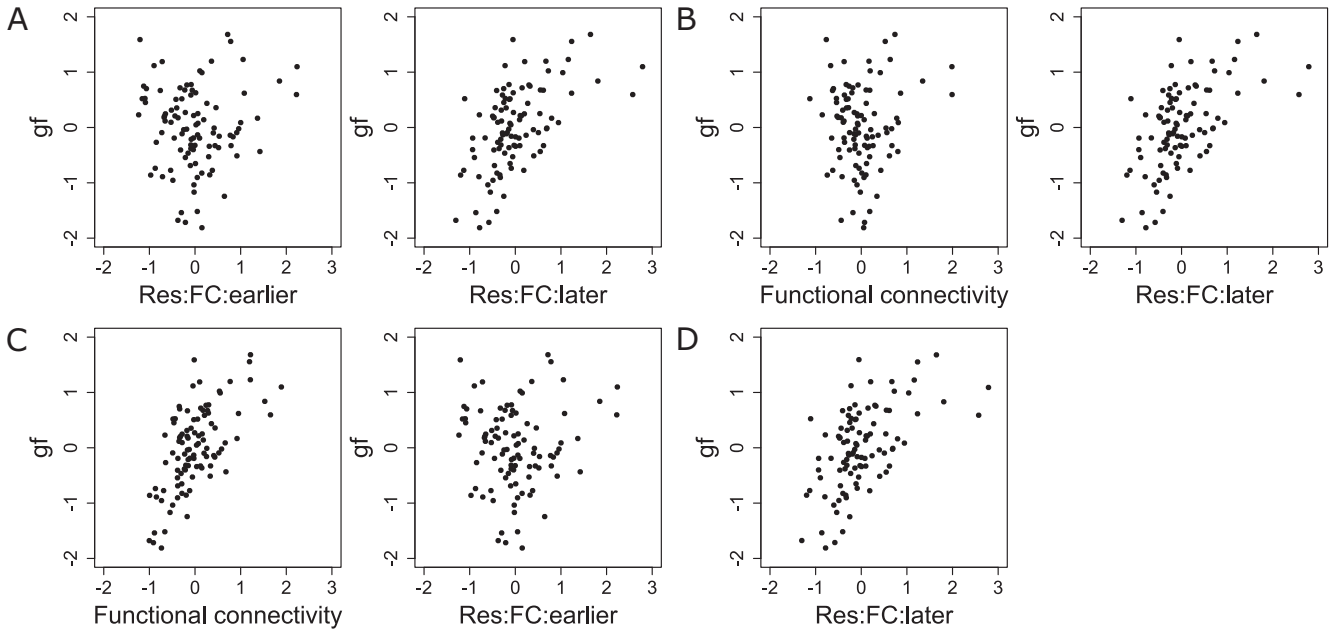
Figure 5. Scatterplots of the latent correlations shown in Figure 3. FC:earlier = functional connectivity during earlier stages of information processing (0–335 ms after stimulus onset); FC:later = functional connectivity during later stages of information processing (335–575 ms after stimulus onset); Res:FC:earlier = residual of the latent FC:earlier variable; Res:FC:later = residual of the latent FC:later variable; *gf* = fluid intelligence. *N* = 98.

regions of interest (e.g., brain areas, electrodes, frequency bands, time windows, etc.) based on psychological theories and to limit data analysis to these prespecified regions of interest. A complimentary more data-driven approach is to define regions of interest based on robust cluster-based permutation testing. To further explore correlations between fluid intelligence and functional connectivity in the theta-band across the time course and different seed regions, we complimented our more theory-driven analyses with data-driven analyses to identify robust Time × Sensor clusters.

Cluster-based permutation testing identified one frontocentral cluster in which the connectivity degree was significantly related to fluid intelligence in the time window from 411 ms to 647 ms after stimulus onset (see Figure 6). This cluster overlapped partly with our a priori specified electrode and time window of interest, but contained also neighboring electrodes (electrodes 1, 2, 5, 6, 7, and 15) and adjacent time points.

Do Individual Differences in Functional Connectivity Reflect Cognitive Control Processes Measured in RTs?

To support our key assumption that individual differences in global theta connectivity reflect cognitive control processes, we subsequently investigated whether functional connectivity during later stages of information processing and reaction speed in the cognitive control task were related and to what degree they predicted individual differences in fluid intelligence. For this purpose, we introduced RTs in the experimental task into the model (see Figure 7A). To model individual differences in RTs, we specified a hierarchical model with lower-order factors of repeat- and shift-

specific variance, and a higher-order factor of reaction time (RT). The overall model provided an acceptable account of the data, $\chi^2(114) = 170.88$, $p < .001$, CFI = .94, RMSEA = 0.07 (95% CI [0.05, 0.09]), but the residual variances of both lower-order RT factors were not significant and one was even negative, all $ps \geq$ .267. Specifying an alternative bifactor model of RTs led to convergence issues. We therefore fixed these variances to zero, which did not impair model fit, $\chi^2(118) = 178.72$, $p < .001$, CFI = .94, RMSEA = 0.07 (95% CI [0.05, 0.09]), $\chi^2_{LLR}(4) = 7.84$, $p = .098$. Individuals with faster RTs also showed greater functional connectivity during later stages of information processing, $r = -.34$, $p = .045$, 95% CI [−.65, −.04], and greater fluid intelligence, $r = -.33$, $p = .006$, 95% CI [−.58, −.08]. See Figure 7B for scatterplots of the three latent correlations.

We then altered the model by regressing both RT and intelligence on functional connectivity (see Figure 7C). This model still provided an acceptable account of the data, $\chi^2(118) = 118.18$, $p < .001$, CFI = .93, RMSEA = 0.08 (95% CI [0.06, 0.10]). When the variance of functional connectivity was partialed out of the relationship between RT and fluid intelligence, their relationship became numerically smaller, but was still statistically significant, $r = -.28$, $p = .025$, 95% CI [−.54, −.01].

We also specified a mediation model to test whether individual differences in functional connectivity mediated the association between RT and intelligence (see Figure 7D). This model provided an acceptable account of the data, $\chi^2(118) = 185.94$, $p < .001$, CFI = .93, RMSEA = 0.08 (95% CI [0.06, 0.10]). The indirect effect of reaction speed on intelligence mediated via functional connectivity was significant, $\beta_{ab} = -.09$, $p = .036$, 95% CI
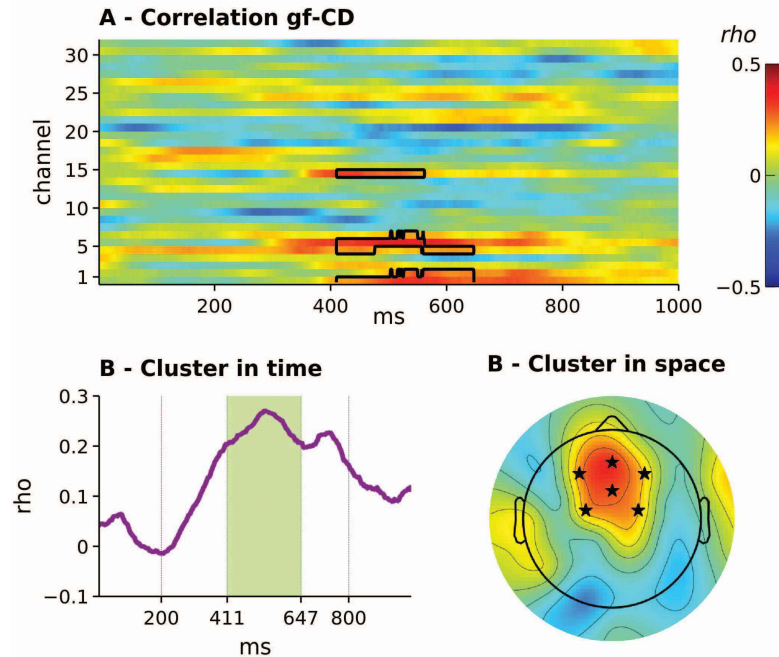
Figure 6. This figure locates the identified significant cluster of correlations between connectivity degree and fluid intelligence. (A) Significant cluster in Time × Sensor space, highlighted by black contour lines. The cluster comprised the electrodes 1, 2, 5, 6, 7, and 15. (B) Time course of correlations of connectivity degree fluid intelligence, averaged across channels belonging to the significant cluster. Here, the cluster in the temporal domain is highlighted by the green rectangle underlying the curve. (C) Topography of correlations averaged across time points included in the significant cluster. The black stars indicate electrodes contained in the significant frontocentral cluster. gf = fluid intelligence; CD = connectivity degree. $N = 97$. See the online article for the color version of this figure.

[−.17, −.01], suggesting that about 25% ($\beta_{ab}/\beta_{total} = −.07/-.28 = .25$) of the association between RT and intelligence was mediated by individual differences in functional connectivity. In addition, RT still predicted variance in fluid intelligence beyond the mediation path, $\beta_{c'} = −.24$, $p = .034$, 95% CI [−.48, −.01]. Taken together, these results suggest that RTs in the cognitive control task and functional connectivity during higher-order processing are linked in their association with intelligence differences, but that there is also specific variance in RTs in the experimental task that is related to intelligence differences and cannot be accounted for by individual differences in functional connectivity.

Do Individual Differences in Functional Connectivity Account for the Association Between P3 Latencies and Fluid Intelligence?

Next, we investigated whether the finding that more intelligent individuals showed shorter P3 latencies (see Figure 3D) might be explained by individual difference in functional connectivity in the theta-band. For this purpose, we introduced P3 latencies as measures of neural processing speed into the model (see Figure 8A). This model provided an excellent account of the data, $\chi^2(116) = 101.60$, $p = .827$, CFI = 1.00, RMSEA = 0.00 (95% CI [0.00, 0.03]). Participants with shorter P3 latencies (i.e., greater neural processing speed) showed both higher intelligence ($r = −.43$, $p = .003$, 95% CI [−.64, −.22]) and greater functional connectivity

during later stages of information processing ($r = −.33$, $p = .026$, 95% CI [−.63, −.03]). See Figure 8B for scatterplots of the three latent correlations.

We then altered the model by regressing both P3 latencies and intelligence on functional connectivity (see Figure 8C). Unsurprisingly, this model also showed a satisfactory model fit, $\chi^2(116) = 109.28$, $p = .658$, CFI = 1.00, RMSEA = 0.00 (95% CI [0.00, 0.04]). When the variance of functional connectivity was partialed out of the relationship between P3 latencies and general intelligence, their relationship remained significant, but became smaller, $r = −.39$, $p = .005$, 95% CI [−.61, −.17].

We also specified a mediation model to test if individual differences in functional connectivity mediated the association between P3 latencies and intelligence (see Figure 8D). This model provided an excellent account of the data, $\chi^2(116) = 108.32$, $p = .681$, CFI = 1.00, RMSEA = 0.00 (95% CI [0.00, 0.04]). The indirect effect of P3 latencies on intelligence mediated via functional connectivity was significant, $\beta_{ab} = −.07$, $p = .038$, 95% CI [−.14, −.00], suggesting that about 18% ($\beta_{ab}/\beta_{total} = −.07/-.17 = .18$) of the association between P3 latencies and intelligence was mediated by individual differences in functional connectivity. Taken together, these results suggest that about a fifth of the association between P3 latencies and general intelligence was explained by individual differences in functional network dynamics.
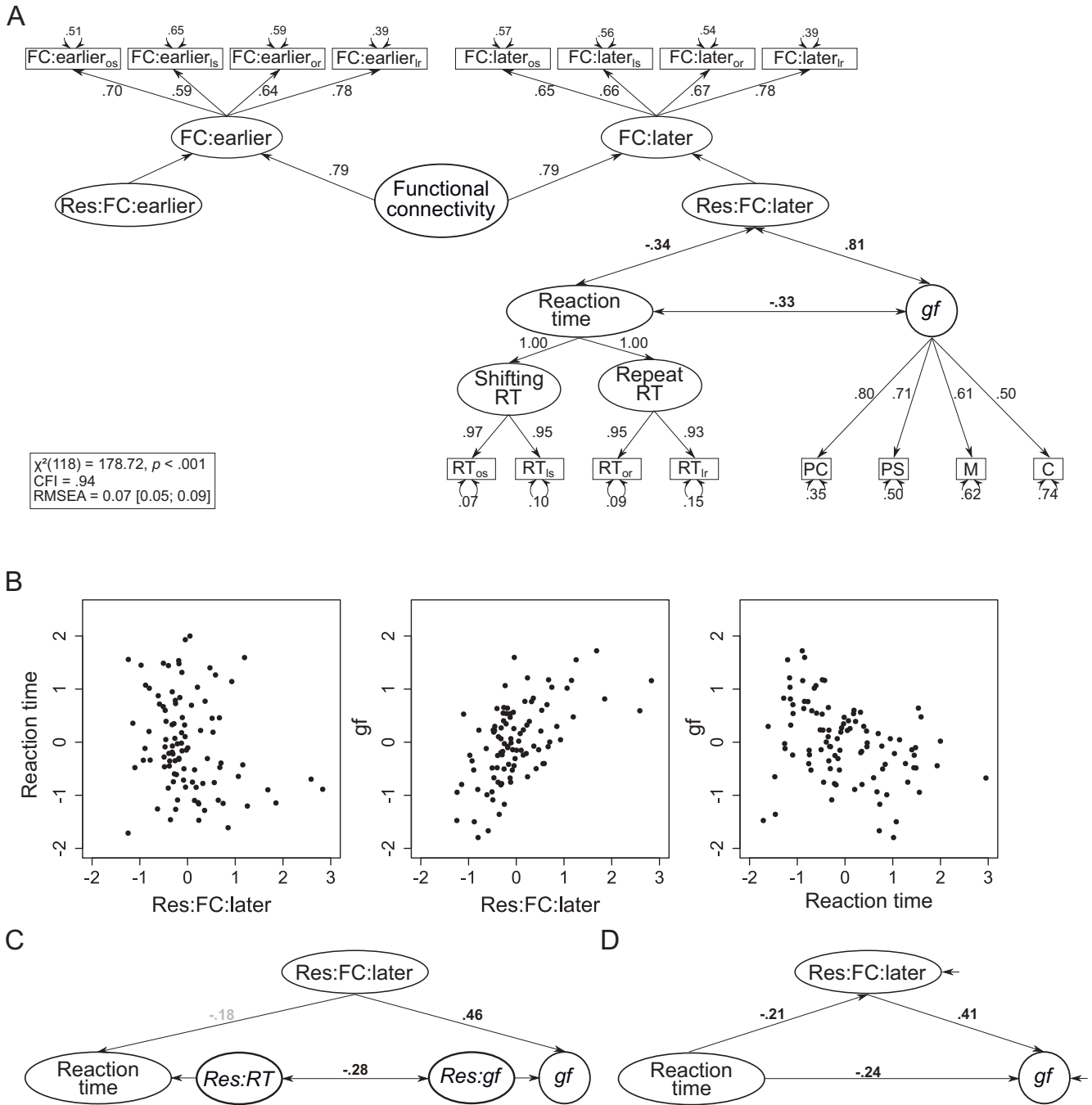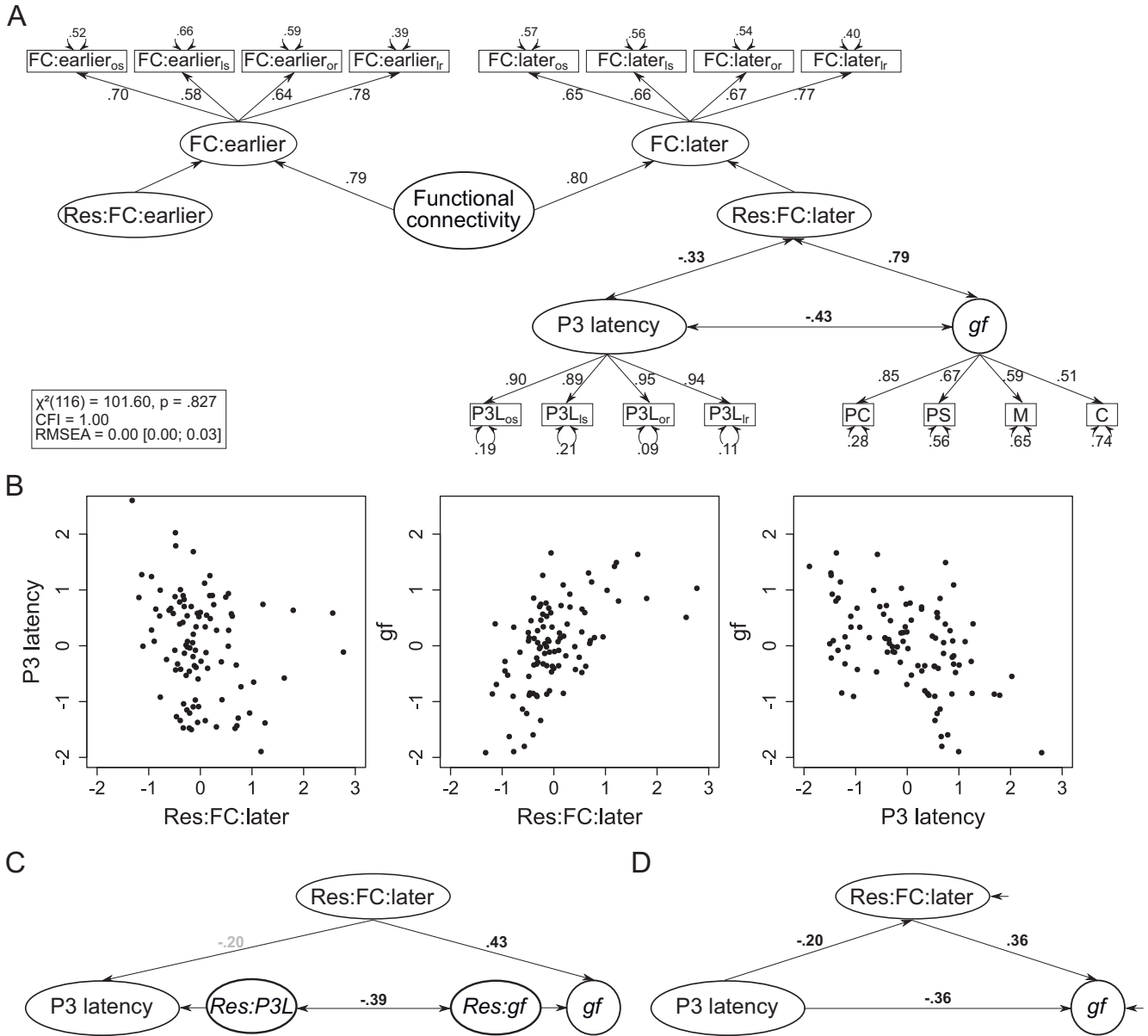
Figure 7. Graphical illustration of three structural equation models of the association between functional connectivity, RT and fluid intelligence. In the model shown in A, correlations between all three measures are estimated freely, with scatterplots of those latent correlations shown in B. The model shown in C is a partial correlation model, and the model shown in D is a mediation model. Standardized regression weights and correlation coefficients are displayed next to paths. Nonsignificant correlations or regressions are grayed out. FC:earlier = functional connectivity during earlier stages of information processing (0–335 ms after stimulus onset); FC:later = functional connectivity during later stages of information processing (335–575 ms after stimulus onset); *gf* = fluid intelligence; Res:FC:earlier: residual of the latent FC:earlier variable; Res:FC:later: residual of the latent FC:later variable; RT = response time; Res: RT: residual of latent RT variable; Res:*gf*: residual of latent fluid intelligence variable; or = odd/even task repeat condition; os = odd/even task shift condition; lr = less/more task repeat condition; ls = less/more task shift condition; PC = processing capacity; PS = processing speed; M = memory; C = creativity. *N* = 98.

Figure 8. Graphical illustration of three structural equation models of the association between functional connectivity, P3 latencies and fluid intelligence. In the model shown in A, correlations between all three measures are estimated freely, with scatterplots of those latent correlations shown in B. The model shown in C is a partial regression model, and the model shown in D is a mediation model. Standardized regression weights and correlation coefficients are shown next to paths. Nonsignificant correlations or regressions are grayed out. FC:earlier = functional connectivity during earlier stages of information processing (0–335 ms after stimulus onset); FC:later = functional connectivity during later stages of information processing (335–575 ms after stimulus onset); *gf* = fluid intelligence; Res:FC:earlier: residual of the latent FC:earlier variable; Res:FC:later: residual of the latent FC:later variable; Res: P3L: residual of latent P3 latency variable; Res:*gf*: residual of latent fluid intelligence variable; or = odd/even task repeat condition; os = odd/even task shift condition; lr = less/more task repeat condition; ls = less/more task shift condition; PC = processing capacity; PS = processing speed; M = memory; C = creativity. *N* = 98.

Are These Results Specific to Functional Connectivity in the Theta-Band?

Finally, we explored whether this time course of the association between functional connectivity and intelligence was unique to the theta-band or could be generalized to other frequency bands. If this were the case, the association between connectivity degrees and intelligence would be less likely to specifically reflect cognitive control functions associated with long-range theta synchronization (Cohen, 2011; Helfrich & Knight, 2016), but instead some

domain-general benefit in information processing. Inspection of both alpha (10 Hz) and delta (2 Hz) frequency synchronization indicated different time-courses of associations between functional connectivity and intelligence for these two frequency bands. In the alpha-band, there was no variance unique to connectivity degrees in the time-window around P3 latencies. More intelligent individuals showed lower functional connectivity at frontal electrodes ($r = -.19$ to $r = -.38$) and greater functional connectivity at parieto-occipital electrodes ($r = .10$ to $r = .39$) across the whole time-course of information processing. In the delta-band, we observed variance unique to connectivity degrees in the time-window around P3 latencies only in a small number of topographically inconsistent electrodes. More intelligent individuals showed lower functional connectivity at central electrodes ($r = -.30$ to $r = -.42$) and greater functional connectivity at lateralized parietal and parieto-occipital electrodes ($r = .18$ to $r = .35$) specifically during the earlier time window (0 – 335 ms). Moreover, they showed lower functional connectivity at lateralized parietal and parieto-occipital electrodes ($r = -.21$ to $r = -.59$) across the whole time-course of information processing (captured in the hierarchical latent variable). Taken together, these results indicate that the chronometry of the observed association between connectivity degrees and intelligence was specific to the theta-band. Because long-range theta synchronization has been shown to underlie cognitive control processes (Cohen, 2011; Helfrich & Knight, 2016), these results therefore indicate that more intelligent individuals benefit specifically from greater functional connectivity underlying controlled processing.

Discussion

Individual differences in task-evoked global theta connectivity at midfrontal electrodes during later stages of higher-order information processing explained 65% of the variance in fluid intelligence. In comparison, task-evoked theta connectivity during earlier stages of information processing was not related to fluid intelligence. Taken together, these results suggest that more intelligent individuals benefit from an adaptive modulation of network dynamics during the time-course of information processing, whereas less intelligent individuals experience a slower and weaker modulation of functional network dynamics. Because long-range theta synchronization plays a crucial role for higher-order cognitive control processes (Cohen, 2011; Helfrich & Knight, 2016), these results support the idea that individual differences in cognitive control during stimulus evaluation give rise to individual differences in intelligence. In particular, our results suggest that, during stages of higher-order processing, more intelligent individuals benefit from an overall greater degree of node centrality in the theta-band, which has been associated with higher-order cognitive control processes (Cohen, 2011; Helfrich & Knight, 2016).

These results are consistent with predictions from the parieto-frontal integration theory of intelligence (P-FIT; Jung & Haier, 2007), which proposes that effective interactions between frontal and parietal brain regions underlie individual differences in intelligence. Because synchronized theta activity has been associated with the coupling of frontoparietal and frontotemporal functional networks (Güntekin & Başar, 2010; Harper et al.,

2017), our results are consistent with neuroimaging studies that found associations between the connectivity of frontoparietal cognitive control networks and intelligence (Cole et al., 2012; Hilger et al., 2017b; Pineda-Pardo et al., 2016; Wendelken et al., 2017) and support the notion that efficient information transmission between these networks contributes to greater intelligence.

However, the present study goes beyond P-FIT by accounting for the temporal dynamics of functional network configurations during the course of information processing. Our core hypothesis was that global functional network dynamics are only—or at least most strongly—related to intelligence when individuals engage in higher-order information-processing. This hypothesis was corroborated in the present study, in which we found correlations between measures of functional connectivity during higher-order processing and intelligence that were greater than most previously reported correlations between functional connectivity and intelligence in neuroimaging research (e.g., Cole et al., 2012; Hilger et al., 2017b; Pineda-Pardo et al., 2016; Wendelken et al., 2017). By considering the time-course of information processing in a cognitive control task, the present study overcomes the limitations of resting-state fMRI data and accounted for the task-evoked elicitation of network dynamics and the suppression of ongoing activity in task-irrelevant areas during attention-regulation (He, 2013).

This greater temporal resolution of intelligence-related functional connectivity comes, however, with a loss of spatial resolution in comparison to fMRI neuroimaging studies. Hence, the present study does not speak to the question of which specific brain area or spatially defined functional network may act as an anatomical correlate of the midfrontal cognitive control hub associated with intelligence. Because our analyses were conducted in sensor space, we cannot claim that the midfrontal cognitive control hub we identified reflects the connectivity degree of midfrontal cortical sources. Owing to the three-dimensional propagation of dipolar fields of each brain region, any activity recorded at head electrodes reflects a summation of all active brain sources modified by their distance, orientation, and the resistivity of various skull tissue compartments (Nunez & Srinivasan, 2006). This is particularly problematic for sensor-based connectivity analyses, because any pair of two sensors can show temporal correlations even though their underlying source activities are temporally unrelated (Schoffelen & Gross, 2009). Therefore, we cannot conclude that the association between connectivity degrees and fluid intelligence identified at the sensor level demonstrates that more intelligent individuals benefit from a greater connectivity between midfrontal and other brain regions. However, despite the limited spatial inferences permitted by the present sensor connectivity analyses, previous studies employing sensor connectivity approaches have linked long-range midline theta connectivity to task processes associated with the frontoparietal cognitive control networks (Güntekin & Başar, 2010; Harper et al., 2017). Future studies using a higher electrode density could go beyond these conclusions by conducting source-level connectivity analyses (Schoffelen & Gross, 2009), which was not feasible in the present study due to the low spatial sampling density of only 32 electrodes (Liu, Ganzetti, Wenderoth, & Mantini, 2018; Ryynänen, Hyttinen, & Malmivuo, 2006; J. Song et al., 2015).

Source-level connectivity analyses would allow to more accurately identify brain areas underlying the cognitive control hub associated with intelligence found in the present study. Because of the advantages of source-level over sensor-level analyses of functional connectivity (Schoffelen & Gross, 2009), it would be very promising for future studies to combine neuroimaging and electrophysiological measurements of cognitive processing or to use source modeling to localize intelligence-related differences in functional connectivity both in time and space. Although volume conduction may have affected our estimates of source-level connectivity, it is still interesting that the association between fluid intelligence and connectivity degrees was specific to frontal seed-electrodes and a time window associated with higher-order processing. To explain such a specific effect of volume conduction, the underlying generators would have to show a complex dipole structure that induced coherence of the sensor time series in such a way that we identified a frontal hub in this specific time window. This specificity of time and topology in our results makes a compelling case for repeating these analyses using a data set with higher electrode density to identify intelligence-related measures of functional connectivity in source space.

Can the Association Between P3 Latencies and Fluid Intelligence Be Attributed to Individual Differences in Functional Network Dynamics?

We found evidence that about 20% of the association between P3 latencies and intelligence could be explained by individual differences in connectivity degrees in the theta band. This result is consistent with previous studies reporting a close link between attention selection and target-related memory updating during the P3 and theta synchronization at frontoparietal and frontotemporal electrode sites (Güntekin & Başar, 2010; Harper et al., 2017). In particular, increases in theta-band connectivity following novel and infrequent targets during an oddball task have been suggested to reflect functional network dynamics underlying the P3 (Harper et al., 2017). However, our results suggest that only some part of the association between P3 latencies and intelligence could be explained by individual differences in functional connectivity, as the correlation between mental speed and mental abilities remained significant after controlling for frontal midline theta connectivity degree. Moreover, individual differences in functional connectivity and in P3 latencies only shared about 11% of variance, suggesting that they measured largely independent neurocognitive processes contributing to human intelligence. Therefore, other genetic, neural, or cognitive processes need to be considered to comprehensively understand the neurocognitive mechanisms underlying the relationship between P3 latencies and general intelligence. This finding is consistent with a watershed model perspective on human intelligence (Kievit et al., 2016), which suggests that fluid intelligence is an observable phenotype that is affected by many small, independent genetic factors that exert their influence on fluid intelligence through a series of intermediate neural and cognitive endophenotypes. Hence, a larger number of underlying neural processes may contribute independently to shorter P3 latencies, which may in turn facil-

itate information processing in working memory and thus affect performance in intelligence tests.

Implications for Theoretical Accounts of Intelligence

By analyzing the chronometry of task-evoked functional connectivity associated with cognitive control, we overcame problems associated with the measurement of individual differences in cognitive control on a behavioral and neurocognitive level. Because our measures did not rely on individual differences in experimental effects and because connectivity degree measures derived from EEG recordings allowed to capture task-evoked fluctuations in functional connectivity with a high temporal resolution, we were able to show that neural correlates of cognitive control processes during stages of higher-order processing explained 65% of the variance in fluid intelligence. To demonstrate the specificity of our results for functional network dynamics associated with controlled processing, we showed that the association between midfrontal global connectivity during stages of higher-order processing and fluid intelligence was specific to the theta-band and did not generalize to other frequency bands that have been associated with different cognitive processes such as the alpha- and delta-band (Cohen, 2011; Helfrich & Knight, 2016). Taken together, we have provided an alternative to the problem-riddled measurement of individual differences in cognitive control that allowed us to find substantial associations between neural correlates of cognitive control and fluid intelligence.

Our results therefore support theoretical accounts of intelligence which suggest that individual differences in cognitive control processes contribute to individual differences in cognitive abilities (Engle, 2018; Kovacs & Conway, 2016, 2019). In particular, our results are consistent with process overlap theory (Kovacs & Conway, 2016), which aims to identify cognitive processes giving rise to individual differences in general intelligence and by doing so bridges the fields of cognitive psychology, individual differences research, and psychometrics. In detail, process overlap theory proposes that domain-general executive processes play a crucial role for individual differences in general intelligence by acting as a bottleneck constraining performance in a great number of cognitive tasks. Our results underline the role of cognitive control processes in human intelligence and demonstrate that more intelligent individuals benefit from a more efficient neural organization of long-range information transmission and from faster neural processing specifically during stages of information-processing associated with higher-order cognitive control processes (Cohen, 2011; Helfrich & Knight, 2016).

Limitations

One limitation of the present study is that both connectivity degrees and P3 latencies were only measured in a single cognitive control task. Previous research has suggested that neurocognitive correlates of intelligence only exhibit trait-like properties (i.e., show temporal stability and transituational consistency) if measured in a wide array of experimental tasks (Schubert, Frischkorn, Hagemann, & Voss, 2016; Schubert et al., 2017). Although first studies on the reliability of graph theoretic measures derived from

EEG reported acceptable test–retest correlations suggesting a high temporal stability (Hardmeier et al., 2014; Kuntzelman & Miskovic, 2017), it is not yet known to what degree these measures contain task-specific and task-invariant portions of variance. Hence, future studies should consider using a broader set of experimental tasks to more reliably capture a consistent and task-invariant measure of functional connectivity in latent variable models.

The shifting task used in the present study was chosen because it is optimally suited for task-related EEG recording and has been successfully used in previous electrophysiological studies to measure functional connectivity between prefrontal and posterior electrode sites (Frischkorn et al., 2019; Sauseng et al., 2006). Individual differences in global theta connectivity in this task are likely to reflect top-down activation and transfer of information between memory systems (Sauseng et al., 2006), resulting from the engagement of executive control processes (Monsell, 2003), the inhibition of interference from persistent task activations (Koch, 2005), the updating of associations between stimulus and response representations (Wylie & Allport, 2000), and/or the updating of event files (Hommel, 2019). These cognitive processes are likely to reflect some of the most elementary components of the concept of cognitive control, but many more tasks that tap into overlapping and different executive processes are available. Because there is currently no consensus regarding the best measures of cognitive control (Draheim, Tsukahara, et al., 2019; Hedge et al., 2018; Paap & Sawi, 2016; Rey-Mermet et al., 2018; Rouder & Haaf, 2019; Schubert & Rey-Mermet, 2019), it would be important to demonstrate that the association between functional connectivity and fluid intelligence found in the present study can be generalized to other measures of cognitive control. One of the most established measures of cognitive control is the antisaccade task, in which participants have to inhibit a prepotent saccade response toward a lateralized cue and make a voluntary saccade to the opposite side to identify a briefly presented target stimulus (Draheim, Tsukahara, et al., 2019; Kane, Bleckley, Conway, & Engle, 2001; Rey-Mermet et al., 2018). Because cue-evoked saccades evoke strong electrophysiological activity (i.e., ocular artifacts) that cannot be easily distinguished from genuine neural activity when locked to cue onset, however, the antisaccade task is ill-suited for electrophysiological studies. Therefore, future studies should employ a diverse set of different cognitive control tasks tapping different executive functions that are suited for electrophysiological research (e.g., flanker task, negative priming task, number-letter task, running span task, keep track task . . .) to evaluate the generalizability of our results.

Moreover, it could be argued that the correlation between connectivity degrees and fluid intelligence may only reflect a correlation between P3 amplitudes and fluid intelligence, as an increase in P3 amplitudes would be associated with greater phase-synchronization spreading out from the seed region due to volume conduction. However, this is unlikely because we calculated connectivity degrees based on the PLI, which is an index defined to be insensitive to volume conduction (see Methods section for details). Moreover, P3 amplitudes were not related to individual differences in connectivity degrees during the relevant time window, $r = .05$, $p = .749$. Therefore, it is very unlikely that individual differences in connectivity degrees reflected individual differences in P3 amplitudes attributable to effects of volume conduction.

Finally, although our sample size was rather large in comparison with other electrophysiological studies and sufficiently powered for the hypothesis of close fit, it was still comparatively small given the complexity of the estimated structural equation models. To assess the robustness of our findings with regard to different model specifications, we refitted all models with factor loadings fixed to 1 and residual variances of observed variables constrained to be equal within each variable domain (i.e., connectivity degrees, intelligence test scores, RTs, P3 latencies) to reduce model complexity. All these parsimoniously specified models provided an excellent account of the data except for one, which (i.e., the one presented in Figure 4A) could not be identified because the covariance matrix of latent variables was not definite positive. Except for this model, all main results closely resembled the results of the more complex models reported in the results section. Although this reanalysis demonstrates the robustness of our findings with regard to model specifications, it is nevertheless important to note that parameter estimates contained a substantial degree of estimation uncertainty as reflected in relatively large confidence intervals. Therefore, point estimates of correlations may have been over- or underestimated. To generate more precise estimates of the effect sizes, it would be important to replicate our results in an independent and ideally larger sample.

Conclusions

Taken together, by considering the chronometry of intelligence-related differences in task-evoked functional connectivity, we have demonstrated that intelligence-related differences in global theta-band synchronization emerged during later stages of higher-order information processing linked to the P3 time window. Individual differences in global theta connectivity at midfrontal electrode sites during this time window explained 65% of the variance in intelligence differences. These results suggest that more intelligent individuals benefit from an adaptive modulation of theta-band synchronization during the time-course of information processing, whereas less intelligent individuals experience a slower and weaker modulation of functional network dynamics. In particular, they suggest that more intelligent individuals benefit from an overall greater degree of node centrality at midfrontal electrodes in the theta-band, which has been associated with higher-order cognitive control processes (Cohen, 2011; Helfrich & Knight, 2016), during stages of higher-order processing. Moreover, they emphasize the role of interregional goal-directed information processing for cognitive control processes in human intelligence and support theoretical accounts of intelligence which suggest that individual differences in cognitive control processes act as a domain-general bottleneck constraining performance in a variety of cognitive ability measures.

Context

The initial idea for this article arose from our search for brain properties that may contribute to the association between neural processing speed and intelligence. In an experimental investigation, we failed to observe a positive effect of nicotine administration on participants' intelligence test scores despite positive effects on the speed of information-processing (Schubert, Hagemann, et al., 2018). We therefore concluded that structural or functional

brain properties may give rise to the substantial association between neural processing speed during stages of higher-order information-processing and intelligence (Schubert et al., 2017). Because P3 latencies have been associated with the efficiency of information transfer from frontal attentional networks to temporal-parietal process of memory storage (Polich, 2007), we decided to investigate the role of attentional and cognitive control processes in intelligence differences and their contribution to the association between neural processing speed and intelligence. Owing to well-known problems with the measurement of cognitive control on a behavioral level (Frischkorn et al., 2019; Gärtner & Strobel, 2019; Hedge et al., 2018; Rey-Mermet et al., 2018, 2019; Rouder & Haaf, 2019), we used midfrontal connectivity degrees in the theta band as a neural correlate of cognitive control with a high temporal resolution.

References

Ackerman, P. L., Beier, M. E., & Boyle, M. O. (2005). Working memory and intelligence: The same or different constructs? *Psychological Bulletin, 131,* 30–60. http://dx.doi.org/10.1037/0033-2909.131.1.30

Barbey, A. K. (2018). Network neuroscience theory of human intelligence. *Trends in Cognitive Sciences, 22,* 8–20. http://dx.doi.org/10.1016/j.tics.2017.10.001

Basten, U., Hilger, K., & Fiebach, C. J. (2015). Where smart brains are different: A quantitative meta-analysis of functional and structural brain imaging studies on intelligence. *Intelligence, 51,* 10–27. http://dx.doi.org/10.1016/j.intell.2015.04.009

Bentler, P. M. (1990). Comparative fit indexes in structural models. *Psychological Bulletin, 107,* 238–246. http://dx.doi.org/10.1037/0033-2909.107.2.238

Booth, T., Bastin, M. E., Penke, L., Maniega, S. M., Murray, C., Royle, N. A., . . . Deary, I. J. (2013). Brain white matter tract integrity and cognitive abilities in community-dwelling older people: The Lothian Birth Cohort, 1936. *Neuropsychology, 27,* 595–607. http://dx.doi.org/10.1037/a0033354

Browne, M. W., & Cudeck, R. (1992). Alternative ways of assessing model fit. *Sociological Methods & Research, 21,* 230–258. http://dx.doi.org/10.1177/0049124192021002005

Burgess, G. C., Gray, J. R., Conway, A. R. A., & Braver, T. S. (2011). Neural mechanisms of interference control underlie the relationship between fluid intelligence and working memory span. *Journal of Experimental Psychology: General, 140,* 674–692. http://dx.doi.org/10.1037/a0024695

Carroll, J. B. (1993). *Human cognitive abilities: A survey of factor-analytic studies.* http://dx.doi.org/10.1017/CBO9780511571312

Chuderski, A. (2014). The relational integration task explains fluid reasoning above and beyond other working memory tasks. *Memory & Cognition, 42,* 448–463. http://dx.doi.org/10.3758/s13421-013-0366-x

Cohen, M. X. (2011). Error-related medial frontal theta activity predicts cingulate-related structural connectivity. *NeuroImage, 55,* 1373–1383. http://dx.doi.org/10.1016/j.neuroimage.2010.12.072

Cohen, M. X. (2014). *Analyzing neural time series data: Theory and practice* (1st ed.). Cambridge, MA: MIT Press Ltd. http://dx.doi.org/10.7551/mitpress/9609.001.0001

Cole, M. W., Yarkoni, T., Repovš, G., Anticevic, A., & Braver, T. S. (2012). Global connectivity of prefrontal cortex predicts cognitive control and intelligence. *The Journal of Neuroscience, 32,* 8988–8999. http://dx.doi.org/10.1523/JNEUROSCI.0536-12.2012

Colom, R., Burgaleta, M., Román, F. J., Karama, S., Álvarez-Linera, J., Abad, F. J., . . . Haier, R. J. (2013). Neuroanatomic overlap between intelligence and cognitive factors: Morphometry methods provide support for the key role of the frontal lobes. *NeuroImage, 72,* 143–152. http://dx.doi.org/10.1016/j.neuroimage.2013.01.032

Colom, R., Jung, R. E., & Haier, R. J. (2007). General intelligence and memory span: Evidence for a common neuroanatomic framework. *Cognitive Neuropsychology, 24,* 867–878. http://dx.doi.org/10.1080/02643290701781557

Colom, R., & Thompson, P. M. (2013). Understanding human intelligence by imaging the brain. In T. Chamorro-Premuzic, S. von Stumm, & A. Furnham (Eds.), *The Wiley-Blackwell handbook of individual differences* (pp. 330–352). London, UK: Wiley/Blackwell. http://dx.doi.org/10.1002/9781444343120.ch12

Deary, I. J., Penke, L., & Johnson, W. (2010). The neuroscience of human intelligence differences. *Nature Reviews Neuroscience, 11,* 201–211. http://dx.doi.org/10.1038/nrn2793

Delorme, A., & Makeig, S. (2004). EEGLAB: An open source toolbox for analysis of single-trial EEG dynamics including independent component analysis. *Journal of Neuroscience Methods, 134,* 9–21. http://dx.doi.org/10.1016/j.jneumeth.2003.10.009

Diamond, A. (2013). Executive functions. *Annual Review of Psychology, 64,* 135–168. http://dx.doi.org/10.1146/annurev-psych-113011-143750

Draheim, C., Mashburn, C. A., Martin, J. D., & Engle, R. W. (2019). Reaction time in differential and developmental research: A review and commentary on the problems and alternatives. *Psychological Bulletin, 145,* 508–535. http://dx.doi.org/10.1037/bul0000192

Draheim, C., Tsukahara, J. S., Martin, J., Mashburn, C., & Engle, R. (2019). *A toolbox approach to improving the measurement of attention control* [Preprint]. http://dx.doi.org/10.31234/osf.io/q985d

Dubois, J., Galdi, P., Paul, L. K., & Adolphs, R. (2018). A distributed brain network predicts general intelligence from resting-state human neuroimaging data. *Philosophical Transactions of the Royal Society B: Biological Sciences, 373,* 20170284. http://dx.doi.org/10.1098/rstb.2017.0284

Engle, R. W. (2018). Working memory and executive attention: A revisit. *Perspectives on Psychological Science: A Journal of the Association for Psychological Science, 13,* 190–193. http://dx.doi.org/10.1177/1745691617720478

Ferrer, E., Whitaker, K. J., Steele, J. S., Green, C. T., Wendelken, C., & Bunge, S. A. (2013). White matter maturation supports the development of reasoning ability through its influence on processing speed. *Developmental Science, 16,* 941–951. http://dx.doi.org/10.1111/desc.12088

Friedman, N. P., & Miyake, A. (2017). Unity and diversity of executive functions: Individual differences as a window on cognitive structure. *Cortex, 86,* 186–204. http://dx.doi.org/10.1016/j.cortex.2016.04.023

Friedman, N. P., Miyake, A., Corley, R. P., Young, S. E., Defries, J. C., & Hewitt, J. K. (2006). Not all executive functions are related to intelligence. *Psychological Science, 17,* 172–179. http://dx.doi.org/10.1111/j.1467-9280.2006.01681.x

Friedman, N. P., Miyake, A., Young, S. E., DeFries, J. C., Corley, R. P., & Hewitt, J. K. (2008). Individual differences in executive functions are almost entirely genetic in origin. *Journal of Experimental Psychology: General, 137,* 201–225. http://dx.doi.org/10.1037/0096-3445.137.2.201

Fries, P. (2005). A mechanism for cognitive dynamics: Neuronal communication through neuronal coherence. *Trends in Cognitive Sciences, 9,* 474–480. http://dx.doi.org/10.1016/j.tics.2005.08.011

Frischkorn, G. T., & Schubert, A.-L. (2018). Cognitive models in intelligence research: Advantages and recommendations for their application. *Journal of Intelligence, 6,* 34. http://dx.doi.org/10.3390/jintelligence6030034

Frischkorn, G. T., Schubert, A.-L., & Hagemann, D. (2019). Processing speed, working memory, and executive functions: Independent or interrelated predictors of general intelligence. *Intelligence, 75,* 95–110. http://dx.doi.org/10.1016/j.intell.2019.05.003

Fuhrmann, D., Simpson-Kent, I. L., Bathelt, J., Kievit, R. A., Holmes, J., Gathercole, S., . . . the CALM Team. (2020). A hierarchical watershed

model of fluid intelligence in childhood and adolescence. *Cerebral Cortex, 30,* 339–352. http://dx.doi.org/10.1093/cercor/bhz091

Gärtner, A., & Strobel, A. (2019). *Individual differences in inhibitory control: A latent variable analysis.* http://dx.doi.org/10.31234/osf.io/gnhmt

Gläscher, J., Rudrauf, D., Colom, R., Paul, L. K., Tranel, D., Damasio, H., & Adolphs, R. (2010). Distributed neural system for general intelligence revealed by lesion mapping. *Proceedings of the National Academy of Sciences of the United States of America, 107,* 4705–4709. http://dx.doi.org/10.1073/pnas.0910397107

Güntekin, B., & Başar, E. (2010). A new interpretation of P300 responses upon analysis of coherences. *Cognitive Neurodynamics, 4,* 107–118. http://dx.doi.org/10.1007/s11571-010-9106-0

Hardmeier, M., Hatz, F., Bousleiman, H., Schindler, C., Stam, C. J., & Fuhr, P. (2014). Reproducibility of functional connectivity and graph measures based on the phase lag index (PLI) and weighted phase lag index (wPLI) derived from high resolution EEG. *PLoS ONE, 9,* e108648. http://dx.doi.org/10.1371/journal.pone.0108648

Harper, J., Malone, S. M., & Iacono, W. G. (2017). Theta- and delta-band EEG network dynamics during a novelty oddball task. *Psychophysiology, 54,* 1590–1605. http://dx.doi.org/10.1111/psyp.12906

Hartmann, E.-M., Rey-Mermet, A., & Gade, M. (2019). Same same but different? Modeling N-1 switch cost and N-2 repetition cost with the diffusion model and the linear ballistic accumulator model. *Acta Psychologica, 198,* 102858. http://dx.doi.org/10.1016/j.actpsy.2019.05.010

Haufe, S., Nikulin, V. V., Müller, K.-R., & Nolte, G. (2013). A critical assessment of connectivity measures for EEG data: A simulation study. *NeuroImage, 64,* 120–133. http://dx.doi.org/10.1016/j.neuroimage.2012.09.036

He, B. J. (2013). Spontaneous and task-evoked brain activity negatively interact. *The Journal of Neuroscience, 33,* 4672–4682. http://dx.doi.org/10.1523/JNEUROSCI.2922-12.2013

Hedge, C., Powell, G., & Sumner, P. (2018). The reliability paradox: Why robust cognitive tasks do not produce reliable individual differences. *Behavior Research Methods, 50,* 1166–1186. http://dx.doi.org/10.3758/s13428-017-0935-1

Helfrich, R. F., & Knight, R. T. (2016). Oscillatory dynamics of prefrontal cognitive control. *Trends in Cognitive Sciences, 20,* 916–930. http://dx.doi.org/10.1016/j.tics.2016.09.007

Hilger, K., Ekman, M., Fiebach, C. J., & Basten, U. (2017a). Efficient hubs in the intelligent brain: Nodal efficiency of hub regions in the salience network is associated with general intelligence. *Intelligence, 60,* 10–25. http://dx.doi.org/10.1016/j.intell.2016.11.001

Hilger, K., Ekman, M., Fiebach, C. J., & Basten, U. (2017b). Intelligence is associated with the modular structure of intrinsic brain networks. *Scientific Reports, 7,* 16088. http://dx.doi.org/10.1038/s41598-017-15795-7

Hommel, B. (2019). Theory of Event Coding (TEC) V2.0: Representing and controlling perception and action. *Attention, Perception, & Psychophysics, 81,* 2139–2154. http://dx.doi.org/10.3758/s13414-019-01779-4

Hu, L., & Bentler, P. M. (1999). Cutoff criteria for fit indexes in covariance structure analysis: Conventional criteria versus new alternatives. *Structural Equation Modeling, 6,* 1–55. http://dx.doi.org/10.1080/10705519909540118

Jäger, A. O., Süß, H.-M., & Beauducel, A. (1997). *Berliner Intelligenzstruktur-Test: BIS-Test, Form 4* [Berlin model of intelligence structure test]. Göttingen, Germany: Hogrefe.

Jewsbury, P. A., Bowden, S. C., & Strauss, M. E. (2016). Integrating the switching, inhibition, and updating model of executive function with the Cattell-Horn-Carroll model. *Journal of Experimental Psychology: General, 145,* 220–245. http://dx.doi.org/10.1037/xge0000119

Jung, R. E., & Haier, R. J. (2007). The Parieto-Frontal Integration Theory (P-FIT) of intelligence: Converging neuroimaging evidence. *Behavioral*

and Brain Sciences, 30, 135–154. http://dx.doi.org/10.1017/S0140525X07001185

Kane, M. J., Bleckley, M. K., Conway, A. R., & Engle, R. W. (2001). A controlled-attention view of working-memory capacity. *Journal of Experimental Psychology: General, 130,* 169–183. http://dx.doi.org/10.1037/0096-3445.130.2.169

Kane, M. J., Hambrick, D. Z., & Conway, A. R. A. (2005). Working memory capacity and fluid intelligence are strongly related constructs: Comment on Ackerman, Beier, and Boyle (2005). *Psychological Bulletin, 131,* 66–71. http://dx.doi.org/10.1037/0033-2909.131.1.66

Kievit, R. A., Davis, S. W., Griffiths, J., Correia, M. M., Cam-Can, & Henson, R. N. (2016). A watershed model of individual differences in fluid intelligence. *Neuropsychologia, 91,* 186–198. http://dx.doi.org/10.1016/j.neuropsychologia.2016.08.008

Kocevar, G., Suprano, I., Stamile, C., Hannoun, S., Fourneret, P., Revol, O., . . . Sappey-Marinier, D. (2019). Brain structural connectivity correlates with fluid intelligence in children: A DTI graph analysis. *Intelligence, 72,* 67–75. http://dx.doi.org/10.1016/j.intell.2018.12.003

Koch, I. (2005). Sequential task predictability in task switching. *Psychonomic Bulletin & Review, 12,* 107–112. http://dx.doi.org/10.3758/BF03196354

Kovacs, K., & Conway, A. R. A. (2016). Process overlap theory: A unified account of the general factor of intelligence. *Psychological Inquiry, 27,* 151–177. http://dx.doi.org/10.1080/1047840X.2016.1153946

Kovacs, K., & Conway, A. R. A. (2019). What is IQ? Life beyond "general intelligence." *Current Directions in Psychological Science, 28,* 189–194. http://dx.doi.org/10.1177/0963721419827275

Kuntzelman, K., & Miskovic, V. (2017). Reliability of graph metrics derived from resting-state human EEG. *Psychophysiology, 54,* 51–61. http://dx.doi.org/10.1111/psyp.12600

Kyllonen, P. C., & Christal, R. E. (1990). Reasoning ability is (little more than) working-memory capacity?! *Intelligence, 14,* 389–433. http://dx.doi.org/10.1016/S0160-2896(05)80012-1

Liu, Q., Ganzetti, M., Wenderoth, N., & Mantini, D. (2018). Detecting large-scale brain networks using EEG: Impact of electrode density, head modeling and source localization. *Frontiers in Neuroinformatics, 12,* 4. http://dx.doi.org/10.3389/fninf.2018.00004

Maris, E., & Oostenveld, R. (2007). Nonparametric statistical testing of EEG- and MEG-data. *Journal of Neuroscience Methods, 164,* 177–190. http://dx.doi.org/10.1016/j.jneumeth.2007.03.024

Miyake, A., & Friedman, N. P. (2012). The nature and organization of individual differences in executive functions: Four general conclusions. *Current Directions in Psychological Science, 21,* 8–14. http://dx.doi.org/10.1177/0963721411429458

Miyake, A., Friedman, N. P., Emerson, M. J., Witzki, A. H., Howerter, A., & Wager, T. D. (2000). The unity and diversity of executive functions and their contributions to complex "Frontal Lobe" tasks: A latent variable analysis. *Cognitive Psychology, 41,* 49–100. http://dx.doi.org/10.1006/cogp.1999.0734

Mognon, A., Jovicich, J., Bruzzone, L., & Buiatti, M. (2011). ADJUST: An automatic EEG artifact detector based on the joint use of spatial and temporal features. *Psychophysiology, 48,* 229–240. http://dx.doi.org/10.1111/j.1469-8986.2010.01061.x

Monsell, S. (2003). Task switching. *Trends in Cognitive Sciences, 7,* 134–140. http://dx.doi.org/10.1016/S1364-6613(03)00028-7

Neisser, U., Boodoo, G., Bouchard, T. J., Jr., Boykin, A. W., Brody, N., Ceci, S. J., . . . Urbina, S. (1996). Intelligence: Knowns and unknowns. *American Psychologist, 51,* 77–101. http://dx.doi.org/10.1037/0003-066X.51.2.77

Nunez, P. L., & Srinivasan, R. (2006). *Electric fields of the brain: The neurophysics of EEG.* Oxford, UK: Oxford University Press.

Oberauer, K., Schulze, R., Wilhelm, O., & Süß, H.-M. (2005). Working memory and intelligence—Their correlation and their relation: Com-

ment on Ackerman, Beier, and Boyle (2005). *Psychological Bulletin, 131,* 61–65. http://dx.doi.org/10.1037/0033-2909.131.1.61

Oostenveld, R., Fries, P., Maris, E., & Schoffelen, J.-M. (2011). FieldTrip: Open source software for advanced analysis of MEG, EEG, and invasive electrophysiological data. *Computational Intelligence and Neuroscience, 2011,* 156869. http://dx.doi.org/10.1155/2011/156869

Paap, K. R., & Sawi, O. (2016). The role of test-retest reliability in measuring individual and group differences in executive functioning. *Journal of Neuroscience Methods, 274,* 81–93. http://dx.doi.org/10.1016/j.jneumeth.2016.10.002

Penke, L., Maniega, S. M., Bastin, M. E., Valdés Hernández, M. C., Murray, C., Royle, N. A., . . . Deary, I. J. (2012). Brain white matter tract integrity as a neural foundation for general intelligence. *Molecular Psychiatry, 17,* 1026–1030. http://dx.doi.org/10.1038/mp.2012.66

Pineda-Pardo, J. A., Martínez, K., Román, F. J., & Colom, R. (2016). Structural efficiency within a parieto-frontal network and cognitive differences. *Intelligence, 54,* 105–116. http://dx.doi.org/10.1016/j.intell.2015.12.002

Polich, J. (2007). Updating P300: An integrative theory of P3a and P3b. *Clinical Neurophysiology, 118,* 2128–2148. http://dx.doi.org/10.1016/j.clinph.2007.04.019

Redick, T. S., Shipstead, Z., Meier, M. E., Montroy, J. J., Hicks, K. L., Unsworth, N., . . . Engle, R. W. (2016). Cognitive predictors of a common multitasking ability: Contributions from working memory, attention control, and fluid intelligence. *Journal of Experimental Psychology: General, 145,* 1473–1492. http://dx.doi.org/10.1037/xge0000219

Rey-Mermet, A., Gade, M., & Oberauer, K. (2018). Should we stop thinking about inhibition? Searching for individual and age differences in inhibition ability. *Journal of Experimental Psychology: Learning, Memory, and Cognition, 44,* 501–526. http://dx.doi.org/10.1037/xlm0000450

Rey-Mermet, A., Gade, M., Souza, A. S., von Bastian, C. C., & Oberauer, K. (2019). Is executive control related to working memory capacity and fluid intelligence? *Journal of Experimental Psychology: General, 148,* 1335–1372. http://dx.doi.org/10.1037/xge0000593

Rosseel, Y. (2012). lavaan: An R package for structural equation modeling. *Journal of Statistical Software, 48,* 1–36. http://dx.doi.org/10.18637/jss.v048.i02

Rouder, J. N., & Haaf, J. M. (2019). A psychometrics of individual differences in experimental tasks. *Psychonomic Bulletin & Review, 26,* 452–467. http://dx.doi.org/10.3758/s13423-018-1558-y

Ryynänen, O. R. M., Hyttinen, J. A. K., & Malmivuo, J. A. (2006). Effect of measurement noise and electrode density on the spatial resolution of cortical potential distribution with different resistivity values for the skull. *IEEE Transactions on Biomedical Engineering, 53,* 1851–1858. http://dx.doi.org/10.1109/TBME.2006.873744

Sauseng, P., Klimesch, W., Freunberger, R., Pecherstorfer, T., Hanslmayr, S., & Doppelmayr, M. (2006). Relevance of EEG alpha and theta oscillations during task switching. *Experimental Brain Research, 170,* 295–301. http://dx.doi.org/10.1007/s00221-005-0211-y

Schmiedek, F., Oberauer, K., Wilhelm, O., Süss, H.-M., & Wittmann, W. W. (2007). Individual differences in components of reaction time distributions and their relations to working memory and intelligence. *Journal of Experimental Psychology: General, 136,* 414–429. http://dx.doi.org/10.1037/0096-3445.136.3.414

Schoffelen, J.-M., & Gross, J. (2009). Source connectivity analysis with MEG and EEG. *Human Brain Mapping, 30,* 1857–1865. http://dx.doi.org/10.1002/hbm.20745

Schubert, A.-L., Frischkorn, G. T., Hagemann, D., & Voss, A. (2016). Trait characteristics of diffusion model parameters. *Journal of Intelligence, 4,* 7. http://dx.doi.org/10.3390/jintelligence4030007

Schubert, A.-L., Hagemann, D., & Frischkorn, G. T. (2017). Is general intelligence little more than the speed of higher-order processing? *Journal of Experimental Psychology: General, 146,* 1498–1512. http://dx.doi.org/10.1037/xge0000325

Schubert, A.-L., Hagemann, D., Frischkorn, G. T., & Herpertz, S. C. (2018). Faster, but not smarter: An experimental analysis of the relationship between mental speed and mental abilities. *Intelligence, 71,* 66–75. http://dx.doi.org/10.1016/j.intell.2018.10.005

Schubert, A.-L., Hagemann, D., Löffler, C., & Frischkorn, G. T. (2020). Disentangling the effects of processing speed on the association between age differences and fluid intelligence. *Journal of Intelligence, 8,* 1. http://dx.doi.org/10.3390/jintelligence8010001

Schubert, A.-L., Hagemann, D., Löffler, C., Rummel, J., & Arnau, S. (2020, April 6). *A chronometric model of the relationship between frontal midline theta functional connectivity and human intelligence.* http://dx.doi.org/10.17605/OSF.IO/VTZAQ

Schubert, A.-L., Hagemann, D., Voss, A., Schankin, A., & Bergmann, K. (2015). Decomposing the relationship between mental speed and mental abilities. *Intelligence, 51,* 28–46. http://dx.doi.org/10.1016/j.intell.2015.05.002

Schubert, A.-L., Nunez, M. D., Hagemann, D., & Vandekerckhove, J. (2018). Individual differences in cortical processing speed predict cognitive abilities: A model-based cognitive neuroscience account. *Computational Brain & Behavior, 2,* 64–84. http://dx.doi.org/10.1007/s42113-018-0021-5

Schubert, A.-L., & Rey-Mermet, A. (2019). Does process overlap theory replace the issues of general intelligence with the issues of attentional control? *Journal of Applied Research in Memory & Cognition, 8,* 277–283. http://dx.doi.org/10.1016/j.jarmac.2019.06.004

Shipstead, Z., Harrison, T. L., & Engle, R. W. (2016). Working memory capacity and fluid intelligence: Maintenance and disengagement. *Perspectives on Psychological Science: A Journal of the Association for Psychological Science, 11,* 771–799. http://dx.doi.org/10.1177/1745691616650647

Smith, E. E., & Jonides, J. (1999). Storage and executive processes in the frontal lobes. *Science, 283,* 1657–1661. http://dx.doi.org/10.1126/science.283.5408.1657

Song, J., Davey, C., Poulsen, C., Luu, P., Turovets, S., Anderson, E., . . . Tucker, D. (2015). EEG source localization: Sensor density and head surface coverage. *Journal of Neuroscience Methods, 256,* 9–21. http://dx.doi.org/10.1016/j.jneumeth.2015.08.015

Song, M., Zhou, Y., Li, J., Liu, Y., Tian, L., Yu, C., & Jiang, T. (2008). Brain spontaneous functional connectivity and intelligence. *NeuroImage, 41,* 1168–1176. http://dx.doi.org/10.1016/j.neuroimage.2008.02.036

Sporns, O. (2011). The human connectome: A complex network. *Annals of the New York Academy of Sciences, 1224,* 109–125. http://dx.doi.org/10.1111/j.1749-6632.2010.05888.x

Sporns, O. (2013). Structure and function of complex brain networks. *Dialogues in Clinical Neuroscience, 15,* 247–262.

Stam, C. J., Nolte, G., & Daffertshofer, A. (2007). Phase lag index: Assessment of functional connectivity from multi channel EEG and MEG with diminished bias from common sources. *Human Brain Mapping, 28,* 1178–1193. http://dx.doi.org/10.1002/hbm.20346

Sudevan, P., & Taylor, D. A. (1987). The cuing and priming of cognitive operations. *Journal of Experimental Psychology, 13,* 89–103. http://dx.doi.org/10.1037/0096-1523.13.1.89

Tamnes, C. K., Østby, Y., Walhovd, K. B., Westlye, L. T., Due-Tønnessen, P., & Fjell, A. M. (2010). Intellectual abilities and white matter microstructure in development: A diffusion tensor imaging study. *Human Brain Mapping, 31,* 1609–1625. http://dx.doi.org/10.1002/hbm.20962

Unsworth, N. (2015). Consistency of attentional control as an important cognitive trait: A latent variable analysis. *Intelligence, 49,* 110–128. http://dx.doi.org/10.1016/j.intell.2015.01.005

Unsworth, N., Redick, T. S., Lakey, C. E., & Young, D. L. (2010). Lapses in sustained attention and their relation to executive control and fluid

abilities: An individual differences investigation. *Intelligence, 38,* 111–122. http://dx.doi.org/10.1016/j.intell.2009.08.002

Unsworth, N., Spillers, G. J., & Brewer, G. A. (2009). Examining the relations among working memory capacity, attention control, and fluid intelligence from a dual-component framework. *Psychology Science, 51,* 388–402.

Verleger, R. (2020). Effects of relevance and response frequency on P3b amplitudes: Review of findings and comparison of hypotheses about the process reflected by P3b. *Psychophysiology.* Advance online publication. http://dx.doi.org/10.1111/psyp.13542

Wendelken, C., Ferrer, E., Ghetti, S., Bailey, S. K., Cutting, L., & Bunge, S. A. (2017). Frontoparietal structural connectivity in childhood predicts development of functional connectivity and reasoning ability: A large-scale longitudinal investigation. *The Journal of Neuroscience, 37,* 8549–8558. http://dx.doi.org/10.1523/JNEUROSCI.3726-16.2017

Wendelken, C., Ferrer, E., Whitaker, K. J., & Bunge, S. A. (2016). Fronto-parietal network reconfiguration supports the development of reasoning ability. *Cerebral Cortex, 26,* 2178–2190. http://dx.doi.org/10.1093/cercor/bhv050

Wongupparaj, P., Kumari, V., & Morris, R. G. (2015). The relation between a multicomponent working memory and intelligence: The roles of central executive and short-term storage functions. *Intelligence, 53,* 166–180. http://dx.doi.org/10.1016/j.intell.2015.10.007

Wylie, G., & Allport, A. (2000). Task switching and the measurement of "switch costs." *Psychological Research, 63,* 212–233. http://dx.doi.org/10.1007/s004269900003